UNIVERSITY OF CALIFORNIA, SAN DIEGO

MicroRNA132/212 mediates the anti-proliferative action of GnRH by down-regulation of SirT-1 in pituitary LbetaT2 Gonadotropes

A Thesis Submitted in partial satisfaction of the requirements
for the degree Master of Science

in

Biology

by

Marin Nishimura

Committee in charge:

Professor Nicholas Webster, Chair
Professor Immo Scheffler, Co-Chair
Professor Elvira Tour

2011

The Thesis of Marin Nishimura is approved, and it is acceptable in quality and form for publication on microfilm and electronically:

_____

_____

Co-chair

_____

Chair

UNIVERSITY OF CALIFORNIA, SAN DIEGO

2011

TABLE OF CONTENTS

LIST OF ABREVIATIONS

AC	Adenylate Cyclase
Ac-p53	acetylated p53
BSA	bovine serum albumin
CREB	cAMP response element binding protein
FBS	fetal bovine serum
GAP	GTPase activating protein
GnRH	gonadotropn releasing hormone
GPCR	G-protein coupled receptor
HPG	hypothalamic-pituitary-gonadal axis
MEK	mitogen activated protein kinase
miRNA	micro RNA
miR-132/212	miR-132 and miR-212
MRE	miRNA recognition element
PLL	poly-L-lysine
TBST	tris-buffered saline with tween-20
Tx	treated, treatment
UCSC	University of California, Santa Cruz
UTR	untranslated Region

ACKNOWLEDGEMENTS

I am forever indebted to all the present and past members of the Webster lab for their warmest support and guidance…

Dr. Shweta Sharma

Dr. Marina Fernandez

Mrs. Jing Li

Dr. Supriya Sen

Dr. Debin Lan

Mr. Devendra Mistry

Mr. Tony Baltazar

and

Mr. Joseph Godoy

Finally, from the formative stages of this thesis to the final draft, I owe an immense debt of gratitude to my supervisor Dr. Nicholas Webster, whose extreme kindness and patience will be remembered always.

To each of the above, I extend my deepest heartfelt appreciation.

ABSTRACT OF THE THESIS

MicroRNA132/212 mediates the anti-proliferative action of GnRH by down-regulation of SirT-1 in pituitary LbetaT2 Gonadotropes

by

Marin Nishimura

Master of Science in Biology

University of California, San Diego, 2011

Professor Nicholas Webster, Chair
Professor Immo Scheffler, Co-Chair

Gonadotropin-releasing hormone (GnRH) plays a vital role in the mammal reproductive system by regulating biosynthesis in the pituitary gonadotrope via a complex signaling pathway and gene network. Small non-coding microRNAs (miRNA) are found to play important roles in post-transcriptional gene regulation of many genes. Previously, it has been shown

that tonic GnRH treatment of LβT2 cells causes cell cycle arrest, leading to subsequent apoptosis. Here, we investigated whether miRNA-132/212, the microRNAs most induced upon GnRH stimulation, mediate the anti-proliferative effect of GnRH on these cells. GnRH treatment for increasing times causes increase in both the transcript and mature forms of miR-132/212 levels as measured by qPCR. This miR-132/212 expression were abolished by pretreatment with the adenylate cyclase inhibitor SQ 22536 and MEK inhibitor U0126. SirT-1 was identified as a putative target of miR-132/212 by miRANDA, TargetScan, and miRacle. Acetylated p53, a substrate of SirT-1 deacetylase, was found to be upregulated as a result of GnRH stimulation. P21, a transcriptional target of p53, was also shown to be upregulated as a result of GnRH treatment. These changes in protein levels and block in cell proliferation were recapitulated by transfection of LβT2 cells by pre-miR-132/212, as well as blocked by transfection with anti-miR-132/212 prior to GnRH stimulation. Taken together, our data suggest a possible mechanism by which gonadotropes utilize microRNAs to synchronise their response to GnRH leading to coordinated gonadotropin release and the possible role of microRNAs in the global regulation of reproduction.

INTRODUCTION

The hypothalamic-pituitary-gonadal (HPG) axis is central to the mammalian reproductive system (1). Fluctuations in the hormones cause changes in the hormones produced by each gland in the axis and has numerous, widespread effects throughout the body. The neurons within the hypothalamus produce gonadotropin releasing hormone (GnRH). GnRH is a tropic peptide hormone, which acts in the anterior pituitary via a specific GnRH receptor (GnRH-R) on the plasma membrane of gonadtotrope cells. There, it triggers the synthesis and secretion of gonadotropins leutinizing hormone (LH) and follicle-stimulating hormone (FSH) (2). These gonadotropins in turn regulate most of the reproductive functions and development of both sexes by controlling the production of gonadal steroids and regulating gametogenic and hormonal functions. For example, LH regulates estrogen synthesis and ovulation in females and androgen synthesis in males. FSH, on the other hand, promotes follicle maturation and estrogen release in females and spermatogonia in males (1).

Physiologically, GnRH is secreted in a pulsatile fashion by hypothalamic neurons into the hypophyseal portal system and thus gonadotrope responsiveness is modulated by both the GnRH concentration and by the frequency or pattern of its delivery (2). Such pulsatile GnRH stimulation of gonadotrophs is required for proper gonadotrope function and in turn

stimulates pulsatile release of LH and FSH into the circulation (3). Furthermore, there is a difference in cell response when cells are exposed to either pulsatile or tonic GnRH stimulation; pulsatile GnRH results in the stimulation of gonadotropin subunit mRNA levels and of LH and FSH secretion, whereas continuous exposure to GnRH down-regulates mRNA levels and secretion (4). In addition, increased frequency of pulsatile hypothalamic GnRH stimulation increases the ratio of secreted LH to FSH (4).

The GnRH receptor (GnRH-R), a member of the seven-transmembrane G protein-coupled receptor (GPCR) family, is a receptor that resides primarily on the cell surface of gonadotrophs and mediates all of the effects of GnRH on the target cells (2, 3). The receptor is associated with G proteins Gs, Gi, and Gq/11 and the binding of GnRH to the receptor has the potential to stimulate a diversity of distinct intracellular signaling cascades (5). One arm of the diverse GnRH intracellular signaling cascades is the Gs activation of adenylate cyclase (AC) which catalyzes the conversion of ATP to 3',5'-cyclic AMP (cAMP) and pyrophosphate. Following this activation of AC, the resulting cAMP acts as a second messenger in activation of cAMP-dependent protein kinase (PKA), which then phosphorylates the activation domain of the transcription factor cAMP response element binding protein (CREB) (6-9). CREB activation is involved in many neuronal processes including neuronal survival, proliferation, differentiation, morphogenesis, and plasticity as well as

addiction and circadian rhythms (10). The other arm of G-protein signaling via Gq/11 induces membrane phospholipid turnover and the subsequent formation of inositol 1,4,5-phosphate (IP3) and diacylglycerol (DAG). This leads to a rapid increase in the intracellular calcium level and the subsequent activation protein kinase C, which results in the activation of many important transcription factors as well as ERK, p38 and JNK (11).

Although there have been studies that reveal many aspects of the complex network of signaling pathways leading to transcriptional regulation in the HPG axis, little is known about post-transcriptional regulation, specifically the role of microRNAs (miRNA). MiRNAs comprise a large family of evolutionarily conserved small non-coding single-stranded RNA molecules of about 21-23 nucleotides that regulate gene expression post-transcriptionally by targeting the 3' untranslated region (3'UTR) of specific mRNA targets (12). Mature miRNAs are processed from precursor molecules (pri-miRNAs), which are transcribed by RNA polymerase II either from independent genes or non-coding introns of protein-coding genes. These pri-miRNAs form hairpin structures which then act as substrates for two members of the RNAse III family of enzymes Drosha and Dicer. The product of Drosha cleavage of approximately 70 nucleotides is known as the pre-miRNA, which is exported to cytoplasm via Exportin 5 where Dicer of the RISC complex processes it into a ~20bp miRNA/miRNA duplex. One strand of this duplex, representing a

mature miRNA, is then incorporated into the miRNA-induced silencing complex (RISC). As a part of this complex, the miRNAs base pair to target mRNAs via the partial complementarity to a sequence located in the 3'UTR of the target mRNA. This nucleotide sequence that is recognized by the miRNA is called the miRNA recognition element (MRE). The seed sequence of the miRNA comprises the first seven nucleotides of the miRNA after the initial adenine and is required for the specific binding to its target (13,14). As a result of the annealing of miRNA to its target sequence, it can ultimately regulate gene expression by inducing cleavage or by repression of productive translation (15). In addition, miRNA targeting can trigger mRNA degradation in a similar process to RNA interference (16).

LβT2 cell line is an immortalized gonadotrope cell line that was generated by tumorigenesis in transgenic mice carrying the rat LHβ subunit regulatory region linked to the SV40 T-antigen oncogene. These LβT2 cells exhibit functional characteristics consistent with those of normal pituitary gonadotropes such as LH secretion via a regulated pathway and changes in GnRH-R and LHβ gene expression in response to signaling by GnRH and steroid hormones. As such, they are also sensitive to GnRH pulses and respond by altering gene expression and LH and FSH secretion accordingly (17, 18).

In vitro studies of pituitary gonadotropes typically involve the tonic treatment of GnRH and it has previously been shown that such GnRH stimulation causes G1/G0 arrest and subsequently apoptosis in LβT2 cells (18, 19). Cell cycle checkpoints are control mechanisms that ensure the fidelity of cell division in eukaryotic cells. The first such checkpoint is located at the end of the cell cycle's G1 phase prior to entry into the replicative S phase, which makes the key decision whether the cell should divide, delay division, or enter a resting stage. In the cell cycle, G0 is a stage in which the cell loses the capacity for subsequent cell division and associated with differentiation of the cell and cessation to proliferation (20). Following the arrest, the cell may be targeted for destruction via apoptosis. Originally identified through its characteristic cytological morphology, apoptosis is a mode of death resulting from activation of caspase cascade that occurs both physiological and pathological circumstances (21).

Many studies have revealed the role of miRNA in post-transcriptional regulation in many physiological functions. Yet, little is known concerning miRNA activity in gonadotropes (22) where much of the GnRH response is mediated via the regulation of gene expression. Here, we investigated whether the GnRH response is regulated by miRNAs. First, we show that GnRH induces the miR-132/212 gene and that SirT-1 is a miR-132/212 target in LβT2 cells. We also show that the p53 and p21 are regulated by GnRH downstream

of SirT-1. Further, we show that the GnRH effects on gene expression and cell cycle arrest are blocked by anti-miR-132/212 and mimicked by pre-miR-132/212. Our data suggests that miR-132/212 may play a vital role in the gonadotope function.

MATERIALS AND METHODS

Materials.

GnRH was purchased from Sigma Chemical Co. (St. Louis, MO). For the experiments with inhibitors, U0126, PD98059, SQ22536, and BAPTA-AM were purchased from EMD Chemicals Inc. (Gibbstown, NJ). Rabbit polyclonal anti-SirT-1, anti-acetylated p53, anti-PUMA, anti-cleaved PARP, and mouse polyclonal anti-total p53 were purchased from Cell Signaling Technology, Inc. (Danvers, MA). Rabbit polyclonal anti-p21 and horseradish peroxidase-linked anti-rabbit and anti-mouse antibodies were purchased from Santa Cruz Biotechnology Inc. (Santa Cruz, CA). DMEM and fetal bovine serum were purchased from Invitrogen (Carlsbad, CA). Pre-mir-132/212, negative control pre-miR, negative control anti-miR were purchased from Ambion, Inc. (Austin, TX). A pair of locked nucleic acid (LNA™) oligonucleotides was designed against miR-132/212 with the following complimentary sequences of CTG(T/G)AGACTGTTA and synthesized and purchased from Exiqon (Vedbaek, Denmark). Apo-ONE Homogeneous Caspase-3/7 Assay and CellTiter 96 Aqueous Non-Radioactive Cell Proliferation Assay (MTS Assay) were purchased from Promega Co. (Madison, WI).

Cell Culture.

LβT2 cells, a gift from Dr. Pam Mellon (UCSD), at passages 13-19 were

maintained in monolayer cultures with DMEM supplemented with 10 % FBS, antibiotics (penicillin/streptomycin), and Gluta-max (Life Technologies, Carlsbad, CA) in a humidified 10 % CO_2 atmosphere at 37 ºC. Cells were plated at a density of $1x10^6$ cells/ml in triplicate in 24-, 12-, and 6-well plates or 6-cm dishes coated with 30 ug/mL poly-L-lysine (Sigma, Pittsburgh, PA). For GnRH treatment experiments, cells were starved in DMEM containing 0.5% FBS, antibiotics (penicillin/streptomycin), and Gluta-max for 17 hours, 24 hours following the plating. Cells were then stimulated with 10 nM GnRH for 0.5 to 48 hours in 0.5% FBS starvation media. For anti-miR-132/212 experiments, cells were transfected with 400 pmol of anti-miR-132/212 per million cells or negative control anti-miR either by electroporation using a Microporator (Life Technologies) at 1300 mV for two 20 ms pulses or by Fugene6 Transfection Reagent (Roche, Piscataway, NY) according to the supplier's protocol. Cells were then plated at a density of $1x10^6$ cells/ml in triplicate in 24-, 12-, and 6-well plates or 6-cm dishes coated with 30 ug/mL poly-L-lysine and starved in 0.5% FBS media for 17 hours. Subsequently, cells were treated with 10nM GnRH for 6 to 48 hours in 0.5% FBS starvation media. For pre-miR experiments, cells were transfected with 200 pmol of pre-miR-132 per million cells or with negative control pre-miR and plated at a density of $1x10^6$ cells/ml in triplicate in 24-, 12-, and 6-well plates or 6-cm dishes coated with 30 ug/mL poly-L-lysine for 6 to 48 h before analysis. For inhibitor experiments, cells were pretreated following the overnight starvation with the

inhibitors U0126 (5 μM), PD98059 (5 μM), or SQ22536 (100 μM) for 1 hour before the 10 nM GnRH stimulation.

Microarray and Quantitative PCR.

For the microarray study, the mRNA was isolated from total RNA using the ribosomal RNA reduction kit (Life Technologies, Carlsbad, CA) and labeled using the NCODE labeling kit (Life Technologies, Carlsbad, CA). RNA from unstimulated cells was labeled with Cy3 and RNA from GnRH stimulated cells with Cy5. Labeled probes were hybridized to NCODE arrays (Life Technologies, Carlsbad, CA) in duplicate. For PCR experiments, total RNA was purified with RNA-Bee (Tel-test, Friendswood, TX) according to manufacturer's protocol and first strand cDNA synthesis was done using the cDNA Reverse Transcription Kit (Applied Biosystems, Foster City, CA). Samples for qPCR were run in 20 mL triplicate reactions on a MJ Research Chromo4 instrument using iTaq SYBR Green Master Mix (Bio-Rad, Hercules CA). Sequence- specific primers for AK006051, SirT-1, Beta-actin, and GAPDH were designed using the Universal Probe Library Assay Design Center (Roche). Mature miRNA expression was quantified using Taqman Micro-RNA Assays (Applied Biosystems, Foster City, CA) for miR-132 and miR-212 and normalized to miR-30c expression, which does not change with GnRH treatment (Table 1). Gene expression levels were calculated after normalization to the housekeeping genes, GAPDH and/or beta-actin, using the

ΔΔCt method and expressed as fold mRNA expression levels with respect to non-treated cells. Error bars are SEM.

Western Blot.

LβT2 cells were washed twice with cold DPBS and lysed on ice with 3X RIPA buffer with protease inhibitor (Stratagene, La Jolla, CA) for 5 minutes. The lysates were collected with scrapers and sonicated to shear the chromosomal DNA to be centrifuged for 10 min at 14,000 rpm, 4°C. Total protein was then quantified using Bio-Rad's DC Protein Assay. Using the quantified concentrations of the samples, either 4X LDS Loading Buffer or 6X Sample Buffer (Life Technologies, Carlsbad, CA) was added to 25 ug of protein from each sample and boiled for 5 min to denature proteins. The protein samples were separated by SDS-PAGE on 8-15% acrylamide gel (BioRad) at 150 V for 1 h, then electrotransferred to polyvinylidene difluoride (PVDF) membranes at 90V for 2 hours (Immobilon-P, Millipore Corp., Bedford, MA). The membranes were blocked with 5% nonfat dried milk or 5% BSA in TBS-Tween (50mM Tris-HCL, pH 7.4, 150mM NaCl, 0.1% Tween-20) for 1 h at room temperature, depending on the blocking buffer used for primary antibody incubation. Blots were incubated with polyclonal primary antibodies in blocking buffer (5% BSA for SirT-1, acetylated p53, and PUMA or 5% nonfat dried milk for total p53, PARP, p21, and βtubulin) overnight at 4 ºC. Following the primary antibody incubation, the blots were then washed 3 times in TBS-

Tween and incubated with horseradish peroxidase linked secondary antibodies followed by chemiluminescent detection using SuperSignal West Pico Chemiluminescent Substrate (Thermo Scientific, Rockford, IL).

Transfection and Knock-Down.

LβT2 cells were transfected with pre-miR-132/212, pre-miR negative control, anti-miR-132/212, and negative control anti-miR by either of the following two methods: by electroporation using the Microporator (two 20ms pulses at 1300mV) or by Fugene6 Transfection. In SirT-1 knockdown experiments, LβT2 cells were transfected with SirT-1 siRNA from Santa Cruz Biotechnology.

CellTiter® 96 Aqueous Nonradioactive Cell Proliferation Assay.

The CellTiter® 96 Aqueous nonradioactive cell proliferation assay is a colorimetric method for determining the number of viable cells in proliferation assays. The assay is composed of solutions of the tetrazolium compound 3-(4,5-dimethylthiazol-2-yl)-5-(3- carboxymethoxyphenyl)-2-(4-sulfophenyl)-2H-tetrazolium (MTS) and the electron coupling reagent phenazine methosulfate; (PMS). MTS is biologically reduced by metabolically active cells into a formazan product that is soluble in tissue culture medium. The absorbance of the formazan at 490 nm is proportional to the mitochondrial activity of the cells in the tissue culture. LβT2 cells were plated onto 24 well plates at 10^6 cells per

mL treated as appropriate and the mitochondrial activity was assessed at 0, 6, 12, and 24 h post treatment using the MTS assay following the manufacturer's protocol. At each time point, 20 uL of MTS reagents were added into each well of the 24 well plate and incubated for an 1.5 h in a humidified 10 % CO2 atmosphere at 37 ºC. Following incubation, content of the each well was transferred to a 96 well plate and the absorbance of the resulting solution was read at 490 nm using microplate reader (Spectra Max 340, Molecular Devices).

Apo-ONE Caspase-3/7 Homogeneous Assay.

The Apo-ONE Caspase-3/7 Homogeneous Assay includes a pro-fluorescent caspase 3/7 substrate with an optimized bifunctional cell lysis/activity buffer. The caspase-3/7 substrate Z-DEVD-R110 is a profluorescent substrate which becomes fluorescent upon cleavage by caspase-3/7. Thus, the amount of fluorescent product is proportional to the casepaes-3/7 cleavage activity present in the sample. 2 x 10^5 LβT2 cells were grown on 24 well plates and either treated with 10 nM GnRH, or transfected with pre-miR or negative control pre-miR, or anti-miR or negative control anti-miR as described previously in 200 uL 0.5%FBS starvation media. At the end of each treatment, 200 ul of the assay reagent was added to each well and the incubated on a plate shaker for 1 h at 350 rpm. Following incubation,

fluorescence was measured in a fluorometer at excitation wavelength of 499 nm and emission 521 nm.

RESULTS

GnRH treatment causes cell cycle arrest and apoptosis in LβT2 cells.

It has been shown previously that tonic GnRH treatment on LβT2 cells for longer than 12 h has anti-proliferative and subsequent apoptotic effects. Serum starvation at 0.5% FBS alone causes minimal cell death and apoptosis, but GnRH stimulation notably increases cell death (Figure 1). As seen, a densely packed monolayer of cells is reduced significantly upon GnRH treatment with an increase in the number of floating cells and membrane blebbing on surviving cells.

In order to quantify the extent of cell death caused by GnRH stimulation, we measured viable cell counts using trypan blue and expressed the results as percentage nonviable cells (Figure 2). Trypan blue is a vital stain that selectively stains nonviable cells with membrane damage due to the negative charge of the chromophore. The extent of cell death expressed in percent nonviable cells increases markedly by 6 h and is maintained to 24 h of tonic GnRH treatment. Untreated cells did not show an increase in non-viable cells.. In order to quantify apoptosis following GnRH stimulation, we stained cells with Annexin V. Consistent with other's findings (14), GnRH treatment increases apoptosis of cells to 52% (+/-12%) versus 18% (+/- 5%) in non-treated cells (Figure 3). Finally, we confirmed this increased apoptosis using the Apo-ONE Homogeneous Caspase-3/7 Apoptosis Assay with different

times of GnRH treatment. As before, GnRH treatment increases apoptosis measured by caspase 3/7 activities by 450% at 12h and 480% at24h compared to non-treated cells and increasing 1200% at 48 h of GnRH(Figure 4).

GnRH stimulation causes upregulations of miR 132/212 in LβT2 cells.

In order to elucidate the mechanisms this block in proliferation occur and at the same time make a connection between GnRH signaling in gonadotropes with post-transcriptional regulation by miRNA, we performed miRNA expression microarray profile on RNA from LβT2 cells following 24 h GnRH treatment (Table 1). Out of 280 miRNAs on the NCODE chip, only 85 were detected in LβT2 cells, most of which were not significantly altered by GnRH treatment. Among the most highly upregulated miRNAs, miR-212 expression was induced 41-fold, and miR-132 was induced 10-fold. (Figure 5) This was verified by qPCR for the mature forms of miR-132/212 (Figure 6). MiR-30c was used as an internal control for LβT2 cells based on the microarray data showing that its expression is unchanged by GnRH.

MiR-132/212 arise from the miR-212/132 cluster located in the intron of the non-protein coding mouse EST AK006051 gene on mouse chromosome 11 (Figure 7). Both microRNAs are highly conserved across vertebrates as is the promoter region. The intron and promoter have CRE consensus sequences directly upstream, and the expression is enhanced by the

transcription factor cAMP-response element binding protein (CREB)(23). It is thought that miR-132 and 212 are derived from the same primary microRNA and share the same seed sequence, indicating that they have the similar target mRNAs. QPCR analysis shows robust induction of the AK006051 transcript starting at 30 min under GnRH treatment (Figure 8). The induction is reduced at 24 hours, although it remains significantly upregulated even at 48 hours. In order to elucidate signaling events upstream of AK006051 induction, we pre-treated cells with the adenylate cyclase inhibitor SQ22536, the MEK inhibitors U0126 or PD89059. Pre-treatment with SQ22536 reduces the GnRH-induced increase in AK006051 mRNA, confirming cAMP-mediated miR-132/212 induction (Figure 8).

miR-132/212 causes downregulation of SirT-1

Among the hundreds of predicted miR-132/212 targets identified by miRANDA, TargetScan, and miRacle, Silent Information Regulator SirT-1 was identified as a potential miR-132/212 target (Tables 2, 3). SirT- 1 is an enzyme that catalyzes deacetylation of acetyl-lysine residues by a mechanism in which NAD+ is cleaved and a unique product, O-acetyl ADP-ribose, is generated (24, 25). Sirt-1 plays a critical role in a wide variety of processes including stress resistance, differentiation, and aging (25). Of the myriad of cellular functions SirT-1 is known to exhibit, it has been shown to interact with and deacetylate the p53 tumor suppressor protein, which is a key transcriptional

regulator of genes involved in cell cycle progression, apoptosis, and DNA repair. P53 becomes acetylated after DNA damage, and the acetylated form increased transcriptional activity, enhanced site-specific DNA binding, and increased stability as the acetylation prevents ubiquitination and subsequent proteasomal degradation. SirT-1 mediated deacetylation of p53, therefore, reduces p53-mediated transcription, preventing cellular senescence and apoptosis induced by DNA damage and stress. (24, 25, 26)

In LβT2 cells both SirT-1 mRNA and protein are reduced upon GnRH stimulation (Figure 9). In order to confirm that miR-132/212 are directly responsible for the degradation of SirT-1, we transfected cells with pre-miR-132 and saw a significant decrease in mRNA after 48 hours (Figure 10A). Transfection of cells with pre-miR-132 also caused decrease in SirT-1 protein levels (Figure 10B). We also transfected cells with a locked nucleic acid (LNA) complimentary to the seed sequences of miR-132/212 or negative control anti-miR for 48 hours prior to 24 hours of GnRH treatment. This abolished the GnRH-induced reduction in SirT-1 mRNA (Figure 10B).

P53 is a tumor suppressing transcription factor that inhibits proliferation and induces apoptosis in response to cellular stress or damage (26) Acetylation of p53 protects it from ubiquitination and is required for the transcriptional activity of p53 (26, 27). SirT-1 has previously been shown to deactylate p53. Thus, we investigated whether acetylation of p53 changes following GnRH stimulation. As expected, GnRH stimulation causes a time

dependent increase in p53 acetylation starting at 6 h. We also see increases in p53 target genes p21 and PUMA (Figure 11). To ensure these cellular responses are caused by miR-121/212, we transfected cells with pre-miR132/212 and saw corresponding increase in acetylated p53 and p21 protein (Figure 12A). Further, we transfected cells with the anti-miR-132/212 or negative control anti-miR for 24 h and treated with GnRH for 6 h and observed that the acetylated p53 and p21 upregulations upon GnRH stimulation was abolished (Figure 12B). Thus, our data taken together suggest that the degradation of SirT-1 is likely to be responsible for the activation of the p53 pathway.

MiR-132/212 mediate GnRH stimulated cell cycle arrest and apoptosis in LβT2 cells.

In order to confirm that miR-132/212 are responsible for the observed cell cycle arrest and apoptosis in LβT2 cells, we transfected LβT2 cells with either pre-miR-132/212 or negative control and compared the number of viable cells using the MTS Assay (Figure 13A) and the activity of caspase3/7 using Apo-ONE Homogenous Caspase3/7 Assay (Figure 13B). As a result, transfection with the pre-miR-132 reduced the number of viable cells and increased caspase 3/7 activities.

Alternatively, we tested the effect of the anti-miR132/212 on GnRH stimulated cell cycle arrest and apoptosis in LβT2 cells. Cells were transfected

either with anti-miR-132/212 or with negative control anti-miR and plated for 24 h prior to 10 nM GnRH treatment for 48 h. Using the MTS assay, we assessed the number of viable cells in proliferation and found that transfection with anti-miR-132/212 blocked GnRH-stimulated lock in proliferation (Figure 14A). Also, measurement of activities of caspase-3/7 with Apo-ONE Homogenous Caspase 3/7 Assay revealed that transfection with anti-miR-132/212 abolished the anti-proliferative effect of GnRH on LβT2 cells (Figure 14B).

DISCUSSION

The transcriptional up-regulation of specific miRNA genes is a potential mechanism by which signal transduction cascade could mediate their cellular functions and various examples of this phenomenon have already been reported in numerous different tissues (28). For example, up-regulation of miR-146a by Toll-like receptors (TLRs) is suggested to play a critical role in negative feedback loops involved in controlling TLR signaling (29). Furthermore, induction of miR-17/92 cluster by interleukin-6 (IL-6) is reported to be responsible for the effect of IL-6 on bone morphogenetic protein receptor 2 (BMPR2) expression (30). In the present study, we reveal that GnRH up-regulates miR-132/212 at least in part to exert its effect on its target LβT2 cell.

Microarray analysis in GnRH stimulated LβT2 cells identified 85 miRNA transcripts that are differentially expressed and also identified miR-132/212 as the most highly induced. Previously, the miR-132/212 gene has been shown to be regulated in several different cell types and miR-132 is emerging as an important regulatory locus in several biological circuits (31). For example, Brain-derived neurotropic factor (BDNF) induces a rapid and prolonged miR-132 response in cortical neurons. Also, miR-132 is found to be enriched in neurons and is transcriptionally regulated by the basic leucine zipper transcription factor cAMP-response element binding protein (CREB) (32). Furthermore, in the suprachasmatic nucleus of the mouse hypothalamus,

which functions as the master-circadian clock, miR-132 is light-inducible and exhibits circadian rhythm of expression, with peak level observed during the subjective day (33). The qPCR results of LβT2 cells for AK006051 containing the miR-132/212 cluster show GnRH-stimulated upregulation of the transcript and the mature form. Further, the levels of the mature forms of miR-132/212 were upregulated and maintained even after the decline of the AK006051 promoter induction. This seems to suggest the importance miR-132/212 may play in properly mediating GnRH response. We have shown that the highly robust induction of AK006051 by GnRH is likely due to adenylate cyclase activation and the cAMP signaling cascade, which confirms the previous studies demonstrating cAMP-dependent increase in miR-132/212 in other cell types and tissues. MiR-132/212 has also been shown to be under the direct control of CREB response elements located upstream of the miR-132/212 sequences. Taking the robust and specific induction of miR132/212 and the potential means by which it could be highly controlled all suggest that miR-132/212 may in fact play a critical role in proper cellular function.

Analysis of the potential list of the miR132/212 targets generated by TargetScan, miRanda, and miRacle yielded SirT-1 as a putative target. The sirtuins are a class of proteins involved in a myriad of cellular functions such as gene silencing, cell cycle control, and apoptosis (34). Of this sirtuin family, SirT-1 is the most well characterized and it has been shown that SirT-1

deactetylates p53 to promote cell survival and binds to other proteins that act in response to DNA damage and oxidative stress (34). Previously, it has been shown that GnRH exerts anti-proliferative action on LβT2 cells but the process of which was still unknown. Thus, we investigated whether or not miR-132/212 mediates the GnRH induced cell cycle arrest via down-regulation of SirT-1.

First, we confirmed that both protein and transcript levels of SirT-1 was reduced after GnRH stimulation. Further, we showed that Pre-miR-132/212 alone reduces the level of the transcripts, and anti-miR-132/212 rescues GnRH-induced degradation of SirT-1. In order to delineate the mechanism by which SirT-1 down-regulation induces block in cell proliferation and ultimately apoptosis in LβT2 cells, we also showed that acetylation of p53, a well-characterized deacetylase target of SirT-1, also increases with GnRH stimulation. This effect is also recapitulated by pre-miR-132/212 transfection and inhibited by transfection with anti-miR-132/212. In addition, p21, a transcriptional target of p53, also accumulated upon GnRH stimulation. This effect was also recapitulated by pre-miR-132/212 transfection as well as blocked by transfection with anti-miR-132/212 prior to GnRH stimulation. These data taken together suggest that GnRH-induced block in proliferation and apoptosis are mediated by SirT-1 down-regulation and caused by the activation of p53 leading to transcriptional up-regulation of p21.

Secondly, we confirmed the anti-proliferative and apoptotic action of GnRH upon LβT2 cells by using various proliferation and apoptosis assays. Trypan blue cell exclusion viability assay, Annexin V staining, Apo-ONE Homogeneous Caspase-3/7 Apoptosis Assay, and CellTiter 96 Non-Radioactive Cell Proliferation Assay all revealed reduced proliferation and subsequent apoptosis following tonic GnRH treatment. Further, pre-miR-132/212 transfection resulted in corresponding block in proliferation and subsequent apoptosis. Transfection with anti-miR-132/212 prior to GnRH stimulation resulted in inhibition of anti-proliferative and apoptotic effects of GnRH on LβT2 cells.

Together with the previous findings, these results suggest that miR-132/212 mediate anti-proliferative and apoptotic action of GnRH in LβT2 cells via down-regulation of SirT-1. Although we studied this occurrence under tonic stimulation of GnRH in static culture and it is improbable that observed apoptosis of gonadotropes occurs *in vivo*, we propose that the miR-132/212 mediated anti-proliferative action of GnRH may have physiological implications. Previous studies in our laboratory have implicated the role of GnRH induced miR-132/212 upregulation in p250RhoGAP suppression leading to establishment of cell-to-cell communication among gonadotropes by growth and maintenance of dendritic spines. Here, by revealing the role miR-132/212 on GnRH induced block in proliferation in LβT2 cells, we point out the

potential importance of the proposed mechanism on the coordination among the gonadotropes *in vivo*. We believe that gonadotorpes enter G0 phase upon GnRH stimulation in order to commit most of the available energy to neurite outgrowth and any amount of locomotion to establish better connection among the cells.

In conclusion, we have demonstrated the role miR-132/212 may play in the GnRH response by pituitary gonadotropes as well as point out the possibility that miR-132/212 may play a vital role in the coordination of the cyclic control of gonadotropin release and ultimately reproductive function.

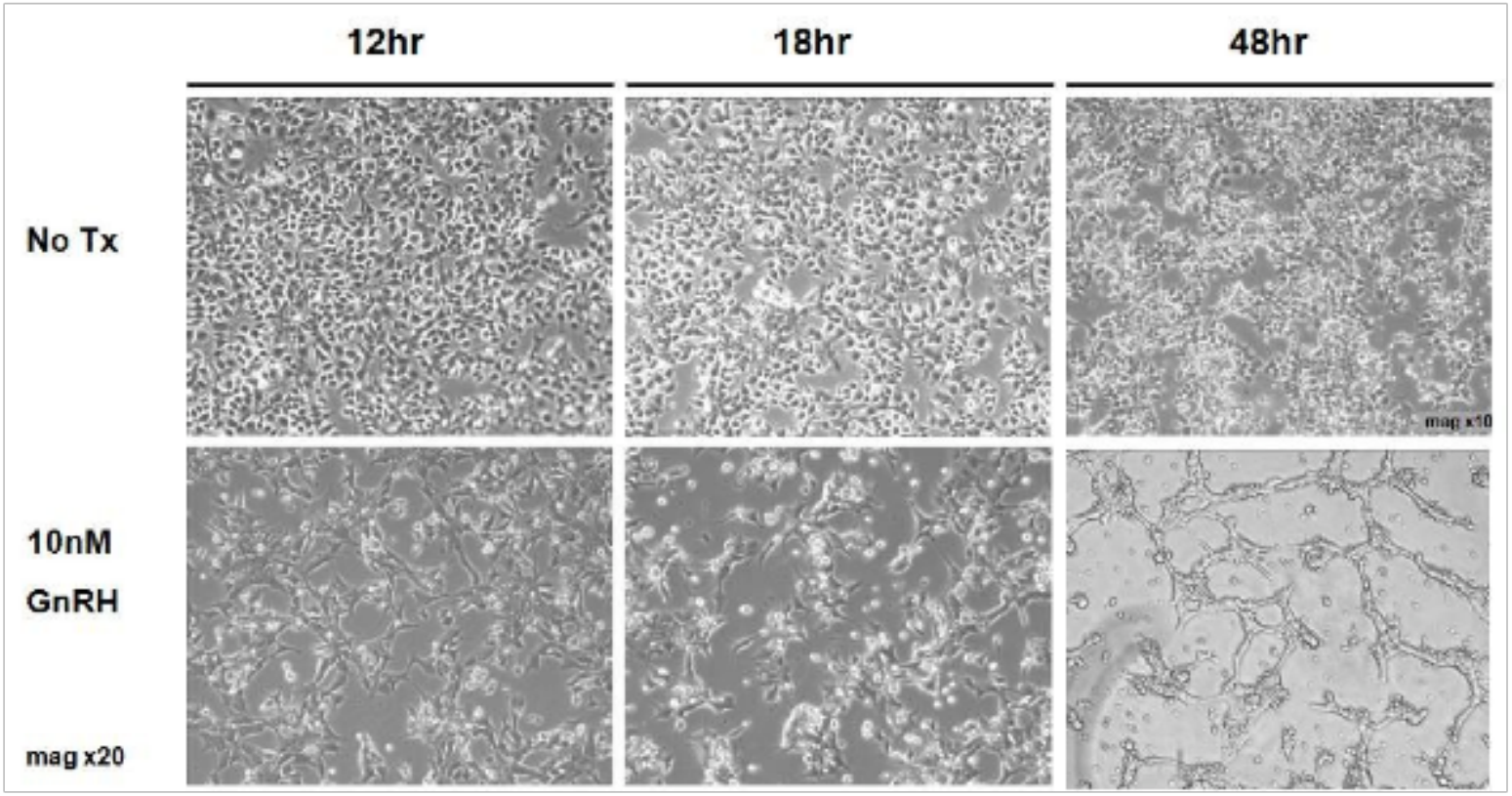

Figure 1. GnRH induces apoptosis in LbetaT2 cells.
LβT2 cells were cultured in monolayers overnight in DMEM containing 10% FBS, antibiotics, and Gluta-Max (Sigma). Cells were then washed once with PBS and starved for 24 hours in DMEM containing 0.5% FBS , antibiotics, an Gluta-Max. Cells were then treated or non-treated by replacing the media with fresh starving media containing 10nM GnRH or not for 12, 18,

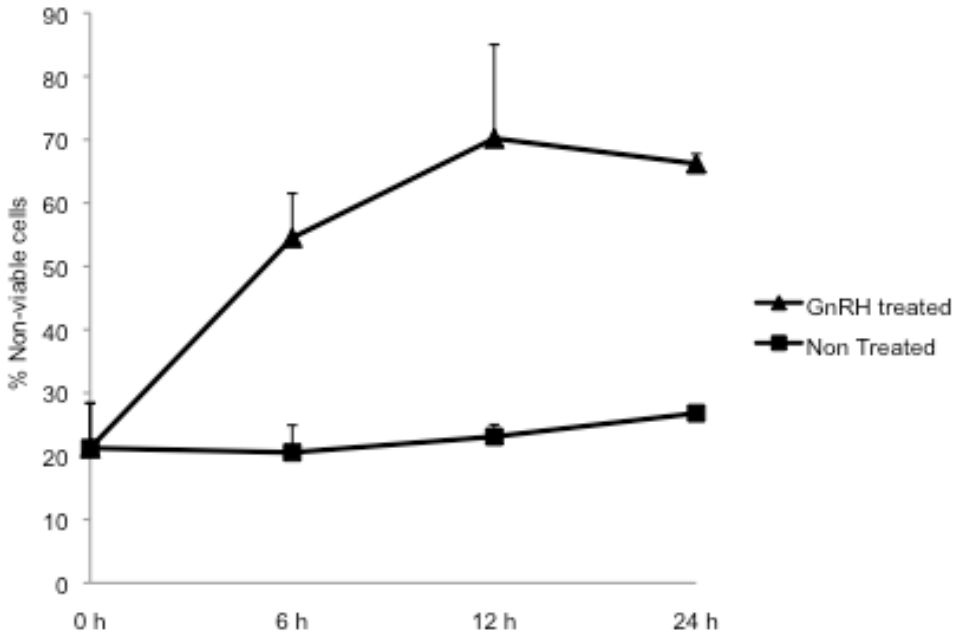

Figure 2. Trypan blue cell exclusion assay of GnRH treated and non-treated cells.
Cells were cultured and subsequently starved overnight before the media was changed to either fresh 0.5% FBS media (non-treated) or 0.5% FBS media with 10 nM GnRH. Cells floating and attached were both counted using hemocytometer to elucidate the cocentration of viable and non-viable cells to calculate the total percent non-viable cells. (n=2)

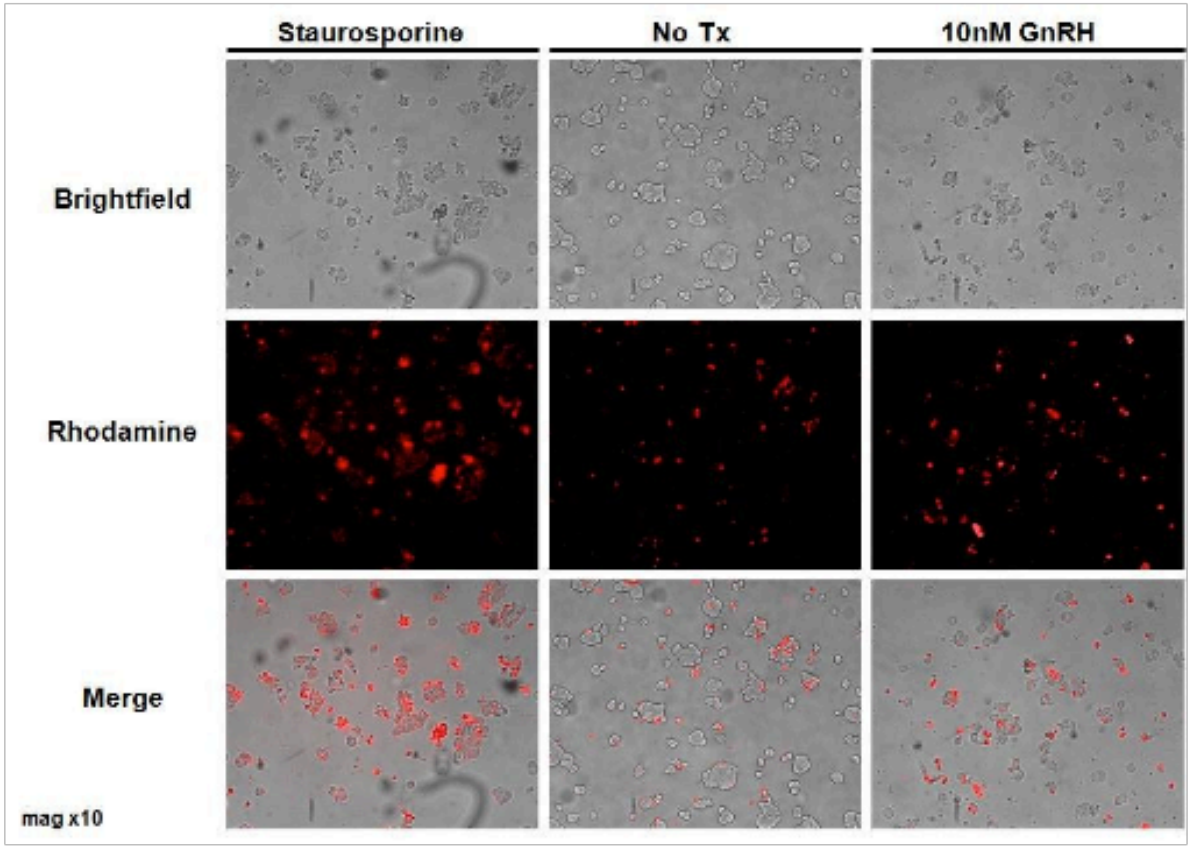

Figure 3. GnRH induces apoptosis.
Cells were cultured in uncoated 6-well plates for 24 hours prior to overnight starvation. Media was then replaced with fresh starvation media with or without 10nM GnRH. The apoptosis inducer staurosporine was added to the media 4 hours prior to Annexin V staining on live cells. Apoptosis/necrosis occurred in 18% of non-treated cells and 52% of treated cells.

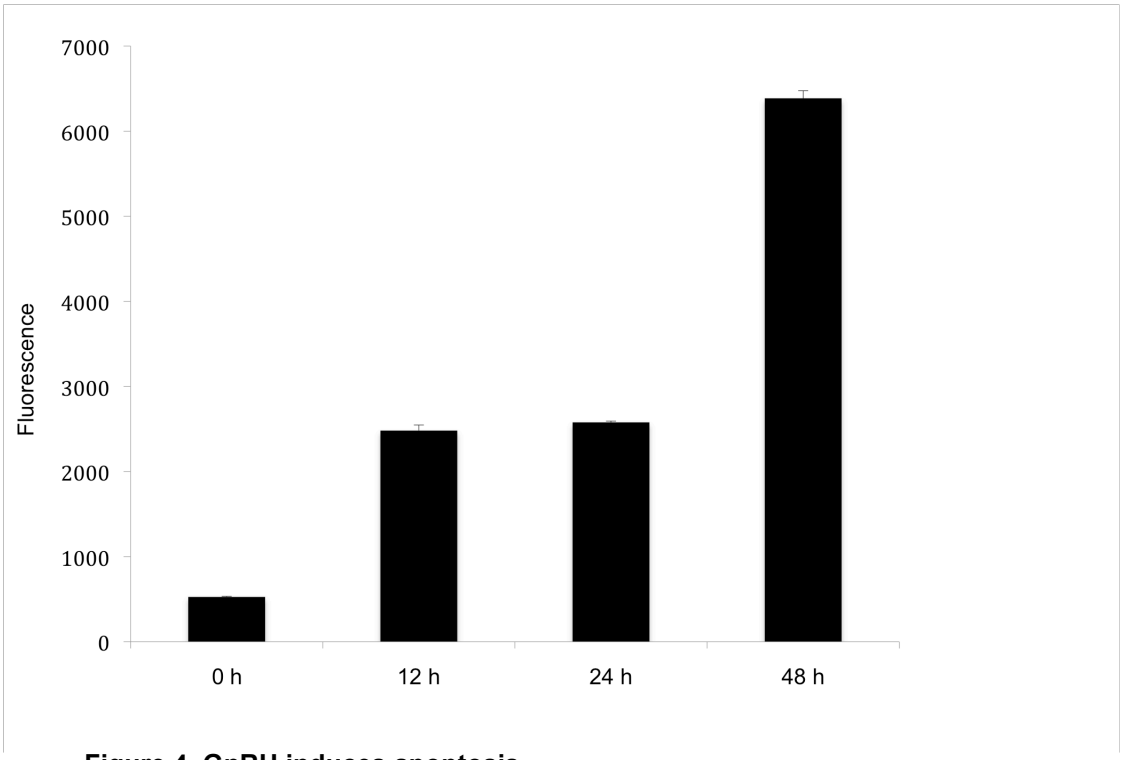

Figure 4. GnRH induces apoptosis.
Cells were cultured on 24 well plates in 10% FBS media and starved in 0.5% FBS media overnight. Media was then changed with either 10 nM GnRH in 0.5% FBS or without. Caspase 3/7 activities were assayed using ApoOne Homogenous Caspase 3/7 Assay. (n=3

Table 1. miRNA exression profile of LβT2 cells.

miRNA ID	Combined Mean ratios 635/532	SD mean ratios	Z-test
01: J-04 2510 mmu miR 99b	0.1265	0.02514624	3.1788E-05
01: J-02 2514 mmu miR 125b	0.2605	0.07135592	2.1881E-01
03: F-08 2597 mmu miR 19b	0.47175	0.37029211	0.0000E+00
01: F-17 C003 Ncode Control	0.47775	0.18035405	6.9879E-04
02: J-18 2530 mmu miR 140*	0.51	0.20334699	2.6351E-03
01: F-18 C003 Ncode Control	0.52775	0.20909228	1.0022E-05
02: N-18 2531 mmu miR 141	0.64275	0.64403125	6.2679E-06
02: B-09 2666 mmu miR 210	0.849	0.61639435	2.2687E-04
01: B-04 2508 mmu miR 30b	0.90175	0.04723258	3.3077E-05
03: J-24 2566 mmu miR 203	0.943	0.63209862	1.8179E-01
03: N-06 2603 mmu miR 200a	1.00275	0.40781481	1.0130E-02
03: B-12 2588 mmu miR 301	1.04725	0.19170355	0.0000E+00
03: J-08 2598 mmu miR 30c	**1.04825**	0.07847452	6.2205E-01
03: N-10 2595 mmu miR 106b	1.128	0.19172376	6.9808E-09
03: N-02 2611 mmu miR 16	1.1375	0.2163739	0.0000E+00
03: J-10 2594 mmu miR 106a	1.1385	0.09210682	2.2221E-03
01: J-18 C004 Ncode Control	1.149	0.27047859	1.9980E-01
01: J-17 C004 Ncode Control	1.1585	0.30061992	1.2568E-13
04: B-24 2612 mmu miR 18	1.161	0.62277711	6.7867E-02
02: F-19 2647 mmu miR 342	1.193	0.78544892	2.4144E-03
01: F-02 2513 mmu miR 125a	1.2165	0.32410441	6.2417E-01
01: J-07 2624 mmu miR 93	1.246	0.38373949	4.4409E-16
01: N-17 C005 Ncode Control	1.30725	0.9824352	2.9166E-01
01: F-01 2635 mmu miR 325	1.3225	0.5415524	2.5436E-10
02: N-06 2555 mmu miR 24	1.35775	0.17236081	2.0741E-02
01: N-18 C005 Ncode Control	1.37125	0.95703165	6.2312E-01
02: J-13 2660 mmu miR 25	1.39225	0.23141215	0.0000E+00
01: B-14 2557 mmu miR 191	1.4225	0.76446648	4.3785E-01
03: J-02 2610 mmu miR 15a	1.4855	0.13949074	2.8978E-04
01: F-09 2619 mmu miR 29a	1.4905	0.32334966	8.5688E-01
01: N-05 2629 mmu miR 103	1.5165	0.29409806	1.9241E-02
03: N-08 2599 mmu miR 30d	1.5725	0.26681642	2.7057E-01
02: F-04 2557 mmu miR 191	1.5805	0.32147628	2.3365E-01
01: F-11 2665 mmu miR 200c	1.60675	0.49027841	3.8044E-06
04: N-24 2615 mmu miR 22	1.61275	1.27905991	7.8576E-02
02: B-24 2516 mmu miR 126 3p	1.617	0.47990485	6.2026E-02
01: J-10 2635 mmu miR 325	1.665	0.36072242	2.3966E-05
01: F-13 1538 mut1 mir 200c	1.6735	0.58322351	1.1502E-04
02: N-02 2563 mmu miR 200b	1.697	0.45573018	3.0447E-04
01: J-06 2506 mmu miR 30a 5p	1.774	0.7672644	2.3050E-03
02: N-24 2519 mmu miR 130a	1.79425	0.43829547	9.8924E-01
02: B-02 2560 mmu miR 195	1.8015	0.34044334	4.4402E-04
02: J-19 2648 mmu miR 344	1.815	0.55432662	2.8485E-05
03: B-08 2596 mmu miR 130b	1.8275	0.79013142	7.6970E-02
02: N-11 2665 mmu miR 200c	1.8395	0.19471432	4.3288E-03

Table 1, Continued

03: B-21 2690_mmu_miR_375	1.93125	1.02005143	3.7137E-09
03: B-07 2718_mmu_miR_429	1.9365	0.15674502	3.3777E-12
01: N-11 2617_mmu_miR_26a	1.941	0.53461575	1.3319E-02
03: B-10 2592_mmu_let_7d	2.031	0.53468184	0.0000E+00
02: N-10 2547_mmu_miR_182	2.07175	0.48531802	0.0000E+00
04: F-24 2613_mmu_miR_20	2.205	0.56836197	3.3800E-01
02: N-04 2559_mmu_miR_194	2.286	1.46218489	1.2474E-01
02: B-21 2642_mmu_miR_148b	2.3685	1.16924548	1.8155E-01
03: F-04 2605_mmu_let_7a	2.369	0.8037989	3.2412E-10
03: N-04 2607_mmu_let_7c	2.38475	1.4718667	5.3165E-01
02: N-13 2661_mmu_miR_28	2.47475	0.84490369	3.2768E-03
03: J-04 2606_mmu_let_7b	2.48475	1.67906708	1.7760E-05
01: B-08 2500_mmu_let_7i	2.588	0.56351457	4.3108E-04
01: J-08 2502_mmu_miR_15b	2.63925	0.78334598	8.0270E-05
03: J-17 2700_mmu_miR_335	2.6865	0.53333823	6.0513E-01
02: F-10 2545_mmu_miR_129_5p	2.7125	0.55498258	2.2327E-05
02: N-15 2657_mmu_miR_17_5p	2.8285	0.91842819	2.6725E-01
02: J-08 2550_mmu_miR_185	2.85	0.88150591	4.3637E-02
01: B-06 2504_mmu_miR_27b	2.91975	0.83073878	2.4947E-06
03: B-02 2608_mmu_let_7e	2.948	1.18981091	2.7004E-05
01: N-08 2503_mmu_miR_23b	2.9505	0.92346215	1.0586E-03
03: F-02 2609_mmu_let_7f	2.96975	0.99896192	1.7399E-08
03: F-23 2687_mmu_miR_361	3.1125	0.36235296	2.6901E-01
01: J-05 2628_mmu_miR_98	3.22875	0.66773117	3.6208E-02
01: B-09 2618_mmu_miR_26b	3.28475	0.56195396	1.4403E-06
02: F-12 2541_mmu_miR_153	3.44675	1.5554805	0.0000E+00
02: F-15 2655_mmu_miR_107	3.45125	0.49530016	2.0375E-01
01: N-10 2499_mmu_let_7g	3.497	0.55032536	2.4624E-11
02: B-08 2548_mmu_miR_183	3.6905	0.72611684	4.8134E-04
01: N-07 2625_mmu_miR_96	4.29325	2.84800718	5.9887E-02
02: J-17 2652_mmu_miR_351	4.3265	1.61040626	2.0912E-02
01: N-09 2621_mmu_miR_27a	4.93375	5.12485098	0.0000E+00
01: J-11 2616_mmu_miR_23a	6.034	3.3033374	1.6554E-03
02: B-05 2674_mmu_miR_320	6.58275	5.94818383	6.5844E-04
02: B-03 2678_mmu_miR_222	7.09275	2.06657742	6.7703E-10
02: F-17 2651_mmu_miR_350	9.62025	2.74234284	6.0501E-02
02: J-22 2522_mmu_miR_132	**10.76825**	1.28805496	3.6079E-05
01: B-03 2630_mmu_miR_424	11.08425	2.41512476	6.8394E-05
02: N-14 2539_mmu_miR_151	20.84575	21.2696586	2.2624E-03
03: J-07	41.11525	40.6137845	4.8217E-02
02: F-09 2667_mmu_miR_212	**41.82925**	26.7431681	0.0000E+00
	median	1.82125	

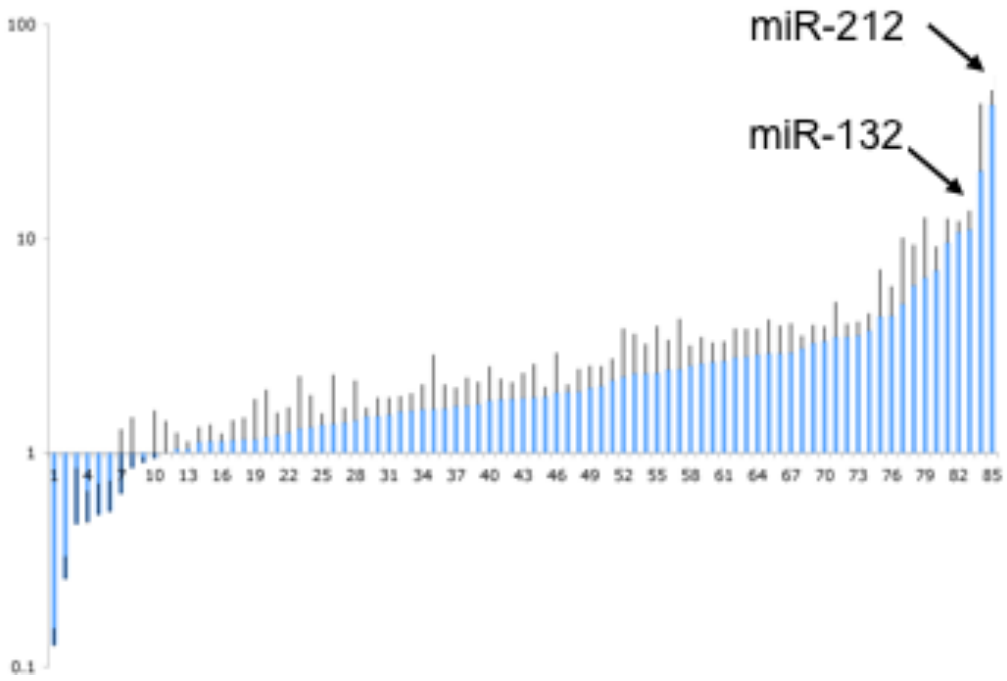

Figure 5. Microarray microRNA profile of LβT2 cells upon GnRH stimulation. As shown, with 24 h 10nM GnRH stimulation, miRNAs 212 and 132 are highly induced.

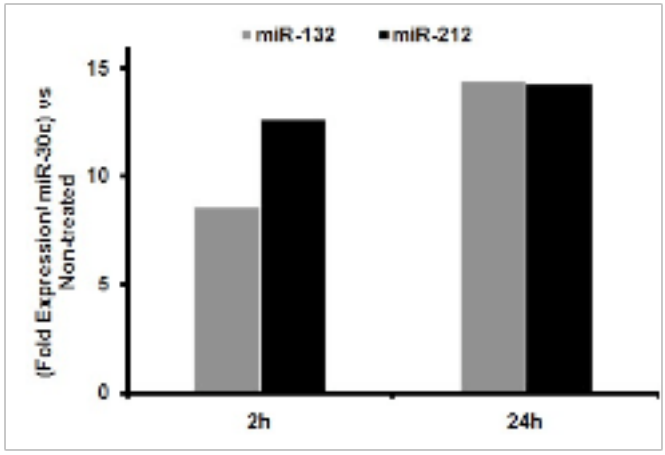

Figure 6. QPCR of mature miR-132/212 induction.
QPCR analysis using TaqMan micro-RNA Assays for mature miR-132 and miR-212. Data is fold expression of each miRNA normalized to non-treated cells. miR-30c was used as the internal control.

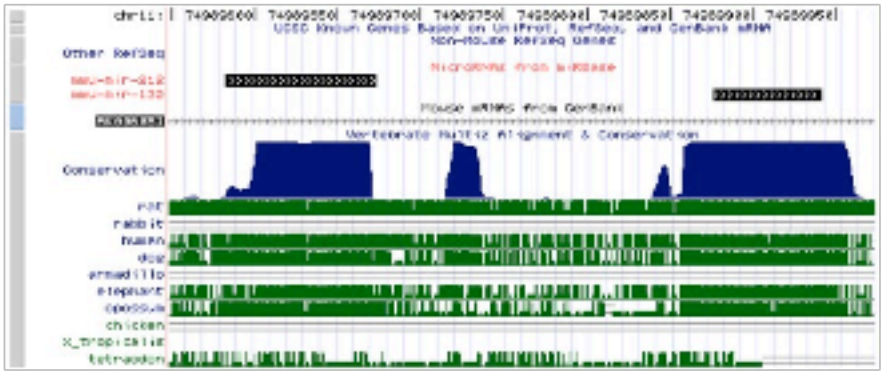

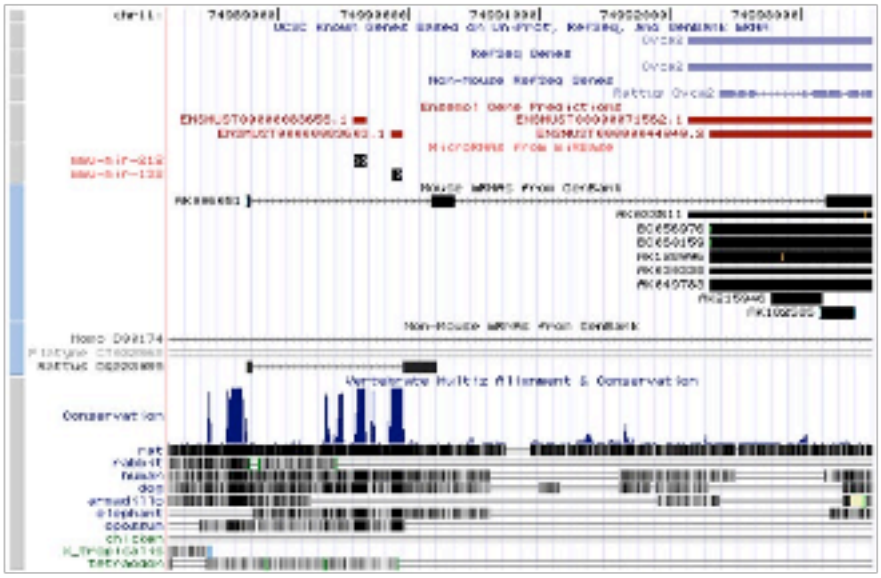

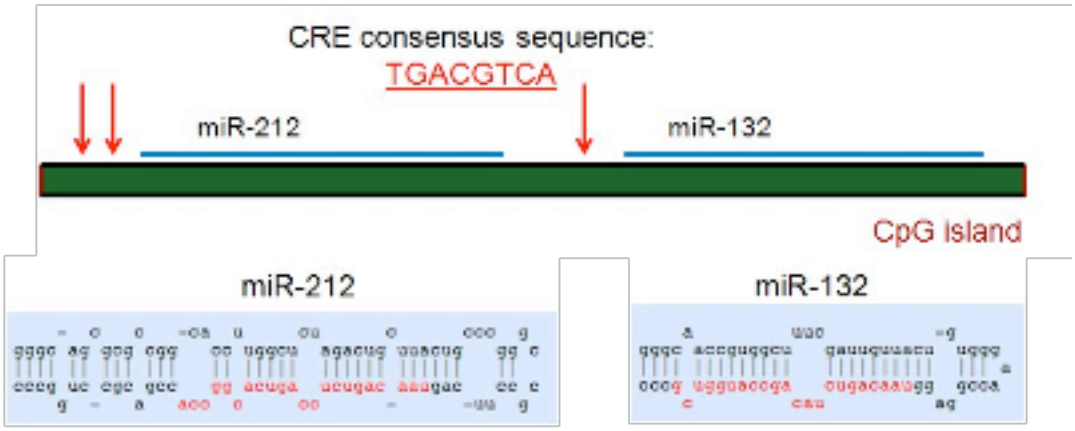

Figure 7. The loci of miR-132/212 in mouse EST AK006051.
Schematic of the loci of miR-132/212 in mouse EST AK006051. The sequence is highly conserved among various vertebrates and both miR132/212 have consensus CRE sites directly upstream.

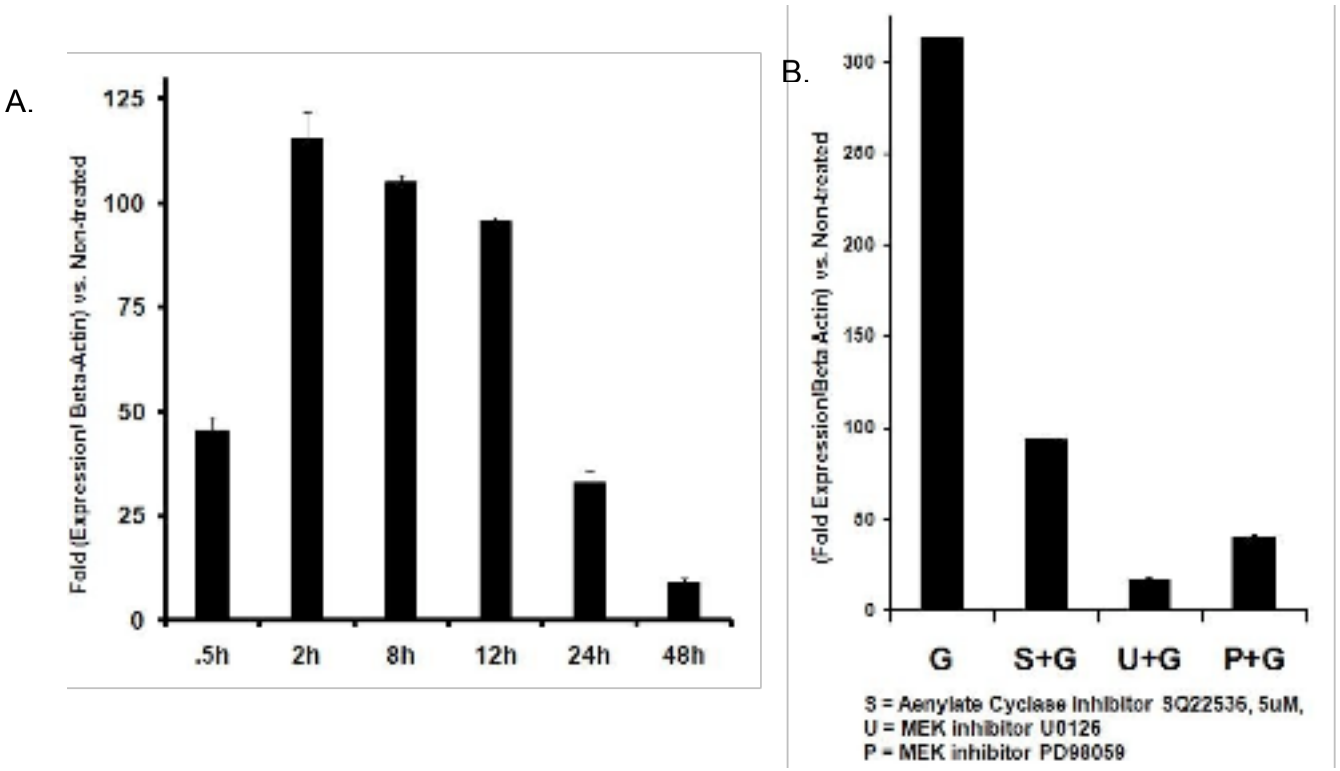

Figure 8. EST AK006051 is induced by GnRH via CREB and ERK.
A. QPCR nalysis using primers flanking the first intron of mouse EST AK006051. Cells were treated with 10nM GnRH for the time courses shown. B. To study signaling events leading to AK006051 induction, cells were pretreated with AC or MEK inhibitors for 1 h prior to 10 nM GnRH stimulation.

Table 2. Potential miR-132/212 Targets Predicted by MiRANDA

Species	Gene Name	Transcript	Description	GO Terms	Total Score	Total Energy	P value	Length	Total Sites	No. Cons Species	No. miRNAs
Mus musculus	Grit	ENSMUST00000047637	Rho GTPase-activating protein [Source:MarkerSymbol;Acc:MGI:2450166]		18.4036	-19.02	1.41005e-10	136	1	9	15 [+]
Mus musculus	Tjap1	ENSMUST00000087020	tight junction associated protein 1 [Source:MarkerSymbol;Acc:MGI:1921344]		18.5229	-23.3	9.42005e-10	542	1	6	54 [+]
Mus musculus	2310022A10Rik	ENSMUST00000067386	RIKEN cDNA 2310022A10 gene (2310022A10Rik), mRNA [Source:RefSeq_dna;Acc:NM_175107]		16.7488	-25.23	6.3567e-08	1257	2	7	23 [+]
Mus musculus	Alkbh3	ENSMUST00000040005	alkB, alkylation repair homolog 3 (E. coli) [Source:MarkerSymbol;Acc:MGI:1916363]		16.5746	-21.54	7.03196e-07	248	1	6	64 [+]
Mus musculus	Grm3	ENSMUST00000004076	glutamate receptor, metabotropic 3 [Source:MarkerSymbol;Acc:MGI:1351340]		16.5267	-15.23	8.83e-07	532	1	9	36 [+]
Mus musculus	Klhl11	ENSMUST00000056665	kelch-like 11 (Drosophila) [Source:MarkerSymbol;Acc:MGI:2388648]		17.3748	-19.4	1.64035e-06	252	2	7	59 [+]
Mus musculus	Paip2	ENSMUST00000041314	polyadenylate-binding protein-interacting protein 2 [Source:MarkerSymbol;Acc:MGI:1915119]		15.8843	-20.46	3.14837e-06	929	1	8	39 [+]
Mus musculus	TIM9_MOUSE	ENSMUST00000050130	Mitochondrial import inner membrane translocase subunit Tim9. [Source:Uniprot/SWISSPROT;Acc:Q9WV98]		17.4793	-14.82	3.4328e-06	379	1	8	52 [+]
Mus musculus	Pdia6	ENSMUST00000057288	protein disulfide isomerase associated 6 [Source:MarkerSymbol;Acc:MGI:1919103]		16.4204	-24.64	4.98048e-06	764	1	8	42 [+]
Mus musculus	Psmd13	ENSMUST00000026560	proteasome (prosome, macropain) 26S subunit, non-ATPase, 13 [Source:MarkerSymbol;Acc:MGI:1345192]		15.4816	-21.12	7.37394e-06	354	1	6	63 [+]
Mus musculus	Mcm2	ENSMUST00000058011	minichromosome maintenance deficient 2 mitotin (S. cerevisiae) [Source:MarkerSymbol;Acc:MGI:105380]		17.623	-21.06	1.36018e-05	524	1	8	48 [+]
Mus musculus	Sqle	ENSMUST00000022977	squalene epoxidase [Source:MarkerSymbol;Acc:MGI:109296]		15.0866	-12.07	1.51043e-05	275	1	6	58 [+]
Mus musculus	Slc25a20	ENSMUST00000035222	solute carrier family 25 (mitochondrial carnitine/acylcarnitine translocase), member 20		15.5583	-25.42	1.54453e-05	747	1	7	37 [+]

Table 3. miR-132/212 targets predicted by TargetScan

Number of conserved targets: 230
Number of conserved sites: 243

Human ortholog of target gene	Gene name	Conserved sites			
		total	8mer	7mer-m8	7mer-1A
NOVA1	neuro-oncological ventral antigen 1	2	1	0	1
SOX5	SRY (sex determining region Y)-box 5	2	1	0	1
OSBPL8	oxysterol binding protein-like 8	2	0	2	0
PRICKLE2	prickle-like 2 (Drosophila)	2	0	2	0
ARID2	AT rich interactive domain 2 (ARID, RFX-like)	2	0	1	1
BTBD7	BTB (POZ) domain containing 7	2	0	1	1
HMGA2	high mobility group AT-hook 2	2	0	1	1
SRGAP3	SLIT-ROBO Rho GTPase activating protein 3	2	0	1	1
TAF4	TAF4 RNA polymerase II, TATA box binding protein (TBP)-associated factor, 135kDa	2	0	1	1
ZNF238	zinc finger protein 238	2	0	1	1
CDC2L6	cell division cycle 2-like 6 (CDK8-like)	2	0	0	2
ST18	suppression of tumorigenicity 18 (breast carcinoma) (zinc finger protein)	2	0	0	2
STX16	syntaxin 16	2	0	0	2
BOLL	bol, boule-like (Drosophila)	1	1	0	0
BRWD1	bromodomain and WD repeat domain containing 1	1	1	0	0
C14orf43	chromosome 14 open reading frame 43	1	1	0	0
C5orf13	chromosome 5 open reading frame 13	1	1	0	0
C8orf13	chromosome 8 open reading frame 13	1	1	0	0
CALU	calumenin	1	1	0	0
CSDE1	cold shock domain containing E1, RNA-binding	1	1	0	0
DAZAP2	DAZ associated protein 2	1	1	0	0
DPYSL3	dihydropyrimidinase-like 3	1	1	0	0
DUSP9	dual specificity phosphatase 9	1	1	0	0
EP300	E1A binding protein p300	1	1	0	0
FLJ36888	hypothetical protein FLJ36888	1	1	0	0
FOXA1	forkhead box A1	1	1	0	0
FOXO3A	forkhead box O3A	1	1	0	0
KCNA6	potassium voltage-gated channel, shaker-related subfamily, member 6	1	1	0	0
LIN28B	lin-28 homolog B (C. elegans)	1	1	0	0
LRRFIP1	leucine rich repeat (in FLII) interacting protein 1	1	1	0	0
LSM11	LSM11, U7 small nuclear RNA associated	1	1	0	0
MAPK1	mitogen-activated protein kinase 1	1	1	0	0
MECP2	methyl CpG binding protein 2 (Rett syndrome)	1	1	0	0
MYCBP2	MYC binding protein 2	1	1	0	0
PAIP2	poly(A) binding protein interacting protein 2	1	1	0	0
PFN2	profilin 2	1	1	0	0
POM121	POM121 membrane glycoprotein (rat)	1	1	0	0
RKHD2	ring finger and KH domain containing 2	1	1	0	0
SEMA4G	sema domain, immunoglobulin domain (Ig), transmembrane domain (TM) and short cytoplasmic domain, (semaphorin) 4G	1	1	0	0
SPPL3	signal peptide peptidase 3	1	1	0	0
SPRED1	sprouty-related, EVH1 domain containing 1	1	1	0	0
SSH2	slingshot homolog 2 (Drosophila)	1	1	0	0
	translocase of inner mitochondrial membrane 9				

Table 3, Continued.

USP9Y	ubiquitin specific peptidase 9, Y-linked (fat facets-like, Drosophila)	1	1	0	0
ZFHX1B	zinc finger homeobox 1b	1	1	0	0
ADAMTS5	ADAM metallopeptidase with thrombospondin type 1 motif, 5 (aggrecanase-2)	1	0	1	0
ADCY3	adenylate cyclase 3	1	0	1	0
AMD1	adenosylmethionine decarboxylase 1	1	0	1	0
ANP32A	acidic (leucine-rich) nuclear phosphoprotein 32 family, member A	1	0	1	0
ARHGEF11	Rho guanine nucleotide exchange factor (GEF) 11	1	0	1	0
ATXN1	ataxin 1	1	0	1	0
BCAN	brevican	1	0	1	0
BCDIN3	bin3, bicoid-interacting 3, homolog (Drosophila)	1	0	1	0
BNC2	basonuclin 2	1	0	1	0
BNIP2	BCL2/adenovirus E1B 19kDa interacting protein 2	1	0	1	0
BRCA1	breast cancer 1, early onset	1	0	1	0
BRI3	brain protein I3	1	0	1	0
BTG2	BTG family, member 2	1	0	1	0
C14orf147	chromosome 14 open reading frame 147	1	0	1	0
C1QL1	complement component 1, q subcomponent-like 1	1	0	1	0
C1orf108	chromosome 1 open reading frame 108	1	0	1	0
C1orf121	chromosome 1 open reading frame 121	1	0	1	0
C6orf106	chromosome 6 open reading frame 106	1	0	1	0
CBX1	chromobox homolog 1 (HP1 beta homolog Drosophila)	1	0	1	0
CFL2	cofilin 2 (muscle)	1	0	1	0
CNIH	cornichon homolog (Drosophila)	1	0	1	0
CREB5	cAMP responsive element binding protein 5	1	0	1	0
DAG1	dystroglycan 1 (dystrophin-associated glycoprotein 1)	1	0	1	0
DEDD	death effector domain containing	1	0	1	0
DNAJA2	DnaJ (Hsp40) homolog, subfamily A, member 2	1	0	1	0
DNAJB14	DnaJ (Hsp40) homolog, subfamily B, member 14	1	0	1	0
EIF4A2	eukaryotic translation initiation factor 4A, isoform 2	1	0	1	0
FAM76B	family with sequence similarity 76, member B	1	0	1	0
FEM1C	fem-1 homolog c (C.elegans)	1	0	1	0
FKBP2	FK506 binding protein 2, 13kDa	1	0	1	0
FLJ45686	No Description	1	0	1	0
GTDC1	glycosyltransferase-like domain containing 1	1	0	1	0
H2AFZ	H2A histone family, member Z	1	0	1	0
H3F3B	H3 histone, family 3B (H3.3B)	1	0	1	0
HMG2L1	high-mobility group protein 2-like 1	1	0	1	0
HN1	hematological and neurological expressed 1	1	0	1	0
HNRPM	heterogeneous nuclear ribonucleoprotein M	1	0	1	0
HNRPU	heterogeneous nuclear ribonucleoprotein U (scaffold attachment factor A)	1	0	1	0
HSPC129	No Description	1	0	1	0
ISL1	ISL1 transcription factor, LIM/homeodomain, (islet-1)	1	0	1	0
KCNJ12	potassium inwardly-rectifying channel, subfamily J, member 12	1	0	1	0
KCNJ2	potassium inwardly-rectifying channel, subfamily J, member 2	1	0	1	0
KCNK2	potassium channel, subfamily K, member 2	1	0	1	0
KIAA0265	KIAA0265 protein	1	0	1	0
KIAA1904	KIAA1904 protein	1	0	1	0
LARGE	like-glycosyltransferase	1	0	1	0

Table 3, Continued.

NFYA	nuclear transcription factor Y, alpha	1	0	1	0
NMNAT2	nicotinamide nucleotide adenylyltransferase 2	1	0	1	0
NR4A2	nuclear receptor subfamily 4, group A, member 2	1	0	1	0
OLFM1	olfactomedin 1	1	0	1	0
PAPOLA	poly(A) polymerase alpha	1	0	1	0
PCDH10	protocadherin 10	1	0	1	0
PCGF3	polycomb group ring finger 3	1	0	1	0
PEA15	phosphoprotein enriched in astrocytes 15	1	0	1	0
PFTK1	PFTAIRE protein kinase 1	1	0	1	0
PHF20L1	PHD finger protein 20-like 1	1	0	1	0
PLXND1	plexin D1	1	0	1	0
PNN	pinin, desmosome associated protein	1	0	1	0
PPM1G	protein phosphatase 1G (formerly 2C), magnesium-dependent, gamma isoform	1	0	1	0
PPP2R5C	protein phosphatase 2, regulatory subunit B (B56), gamma isoform	1	0	1	0
PRPF4B	PRP4 pre-mRNA processing factor 4 homolog B (yeast)	1	0	1	0
PSMD12	proteasome (prosome, macropain) 26S subunit, non-ATPase, 12	1	0	1	0
PTBP2	polypyrimidine tract binding protein 2	1	0	1	0
PURB	purine-rich element binding protein B	1	0	1	0
PXN	paxillin	1	0	1	0
ProSAPiP1	ProSAPiP1 protein	1	0	1	0
RAB15	RAB15, member RAS onocogene family	1	0	1	0
RASA1	RAS p21 protein activator (GTPase activating protein) 1	1	0	1	0
RDX	radixin	1	0	1	0
RICS	**Rho GTPase-activating protein**	1	0	1	0
RKHD3	ring finger and KH domain containing 3	1	0	1	0
SAP30L	No Description	1	0	1	0
SCN3A	sodium channel, voltage-gated, type III, alpha	1	0	1	0
SEMA6A	sema domain, transmembrane domain (TM), and cytoplasmic domain, (semaphorin) 6A	1	0	1	0
SEPHS1	selenophosphate synthetase 1	1	0	1	0
SIRT1	**sirtuin (silent mating type information regulation 2 homolog) 1 (S. cerevisiae)**	1	0	1	0
SLC30A6	solute carrier family 30 (zinc transporter), member 6	1	0	1	0
SLC6A1	solute carrier family 6 (neurotransmitter transporter, GABA), member 1	1	0	1	0
SOX11	SRY (sex determining region Y)-box 11	1	0	1	0
SOX4	SRY (sex determining region Y)-box 4	1	0	1	0
SPRY1	sprouty homolog 1, antagonist of FGF signaling (Drosophila)	1	0	1	0
TAF15	TAF15 RNA polymerase II, TATA box binding protein (TBP)-associated factor, 68kDa	1	0	1	0
TCF7L1	transcription factor 7-like 1 (T-cell specific, HMG-box)	1	0	1	0
TMEFF1	transmembrane protein with EGF-like and two follistatin-like domains 1	1	0	1	0
TRIM2	tripartite motif-containing 2	1	0	1	0
TSC22D3	TSC22 domain family, member 3	1	0	1	0
WHSC1L1	Wolf-Hirschhorn syndrome candidate 1-like 1	1	0	1	0
WT1	Wilms tumor 1	1	0	1	0
YWHAG	tyrosine 3-monooxygenase/tryptophan 5-monooxygenase activation protein, gamma polypeptide	1	0	1	0
ZCCHC11	zinc finger, CCHC domain containing 11	1	0	1	0
ZNF644	zinc finger protein 644	1	0	1	0
A2BP1	ataxin 2-binding protein 1	1	0	0	1
ACHE	acetylcholinesterase (Yt blood group)	1	0	0	1
ACSL4	acyl-CoA synthetase long-chain family member 4	1	0	0	1
ADAMTS6	ADAM metallopeptidase with thrombospondin type 1 motif, 6	1	0	0	1

Table 3, Continued.

ARHGAP27	Rho GTPase activating protein 27	1	0	0	1
ARMC1	armadillo repeat containing 1	1	0	0	1
BICD2	bicaudal D homolog 2 (Drosophila)	1	0	0	1
BSN	bassoon (presynaptic cytomatrix protein)	1	0	0	1
C17orf42	chromosome 17 open reading frame 42	1	0	0	1
C18orf25	chromosome 18 open reading frame 25	1	0	0	1
CACNB4	calcium channel, voltage-dependent, beta 4 subunit	1	0	0	1
CBFA2T2	core-binding factor, runt domain, alpha subunit 2; translocated 2	1	0	0	1
CD164	CD164 antigen, sialomucin	1	0	0	1
CHES1	checkpoint suppressor 1	1	0	0	1
CITED2	Cbp/p300-interacting transactivator, with Glu/Asp-rich carboxy-terminal domain, 2	1	0	0	1
COLQ	collagen-like tail subunit (single strand of homotrimer) of asymmetric acetylcholinesterase	1	0	0	1
CPEB4	cytoplasmic polyadenylation element binding protein 4	1	0	0	1
DACH1	dachshund homolog 1 (Drosophila)	1	0	0	1
DNMT3A	DNA (cytosine-5-)-methyltransferase 3 alpha	1	0	0	1
EIF2C2	eukaryotic translation initiation factor 2C, 2	1	0	0	1
FLJ10357	hypothetical protein FLJ10357	1	0	0	1
FLJ22833	No Description	1	0	0	1
FLJ31818	hypothetical protein FLJ31818	1	0	0	1
FLJ45803	FLJ45803 protein	1	0	0	1
FMR1	fragile X mental retardation 1	1	0	0	1
FOXP1	forkhead box P1	1	0	0	1
FUSIP1	FUS interacting protein (serine/arginine-rich) 1	1	0	0	1
GATA2	GATA binding protein 2	1	0	0	1
GMFB	glia maturation factor, beta	1	0	0	1
GNA12	guanine nucleotide binding protein (G protein) alpha 12	1	0	0	1
GNB1	guanine nucleotide binding protein (G protein), beta polypeptide 1	1	0	0	1
HAO1	hydroxyacid oxidase (glycolate oxidase) 1	1	0	0	1
HBEGF	heparin-binding EGF-like growth factor	1	0	0	1
HIC2	hypermethylated in cancer 2	1	0	0	1
HNRPH1	heterogeneous nuclear ribonucleoprotein H1 (H)	1	0	0	1
HS2ST1	heparan sulfate 2-O-sulfotransferase 1	1	0	0	1
ITGA9	integrin, alpha 9	1	0	0	1
ITPKB	inositol 1,4,5-trisphosphate 3-kinase B	1	0	0	1
KIAA0240	KIAA0240	1	0	0	1
LASS2	LAG1 longevity assurance homolog 2 (S. cerevisiae)	1	0	0	1
LIN9	lin-9 homolog (C. elegans)	1	0	0	1
LOC401498	similar to RIKEN A930001M12	1	0	0	1
LOC93081	No Description	1	0	0	1
MEGF11	MEGF11 protein	1	0	0	1
MEIS1	Meis1, myeloid ecotropic viral integration site 1 homolog (mouse)	1	0	0	1
MGC17330	HGFL gene	1	0	0	1
MGC48972	No Description	1	0	0	1
MYST2	MYST histone acetyltransferase 2	1	0	0	1
NET1	neuroepithelial cell transforming gene 1	1	0	0	1
NFAT5	nuclear factor of activated T-cells 5, tonicity-responsive	1	0	0	1
NLK	nemo-like kinase	1	0	0	1
OSBPL11	oxysterol binding protein-like 11	1	0	0	1

Table 3, Continued.

RAB28	RAB28, member RAS oncogene family	1	0	0	1
RAB6B	RAB6B, member RAS oncogene family	1	0	0	1
RTN4	reticulon 4	1	0	0	1
SATB2	SATB family member 2	1	0	0	1
SFRS1	splicing factor, arginine/serine-rich 1 (splicing factor 2, alternate splicing factor)	1	0	0	1
SOX2	SRY (sex determining region Y)-box 2	1	0	0	1
TCEB1	transcription elongation factor B (SIII), polypeptide 1 (15kDa, elongin C)	1	0	0	1
TCF7L2	transcription factor 7-like 2 (T-cell specific, HMG-box)	1	0	0	1
TLN2	talin 2	1	0	0	1
TLOC1	translocation protein 1	1	0	0	1
TMEM2	transmembrane protein 2	1	0	0	1
TRIB2	tribbles homolog 2 (Drosophila)	1	0	0	1
UBE2D3	ubiquitin-conjugating enzyme E2D 3 (UBC4/5 homolog, yeast)	1	0	0	1
USP15	ubiquitin specific peptidase 15	1	0	0	1
USP6	ubiquitin specific peptidase 6 (Tre-2 oncogene)	1	0	0	1
VAPA	VAMP (vesicle-associated membrane protein)-associated protein A, 33kDa	1	0	0	1
VDAC2	voltage-dependent anion channel 2	1	0	0	1
WDR42A	WD repeat domain 42A	1	0	0	1
ZFYVE1	zinc finger, FYVE domain containing 1	1	0	0	1
ZHX1	zinc fingers and homeoboxes 1	1	0	0	1
ZNF207	zinc finger protein 207	1	0	0	1
ZNF365	zinc finger protein 365	1	0	0	1
ZNF395	zinc finger protein 395	1	0	0	1
ZNF650	zinc finger protein 650	1	0	0	1

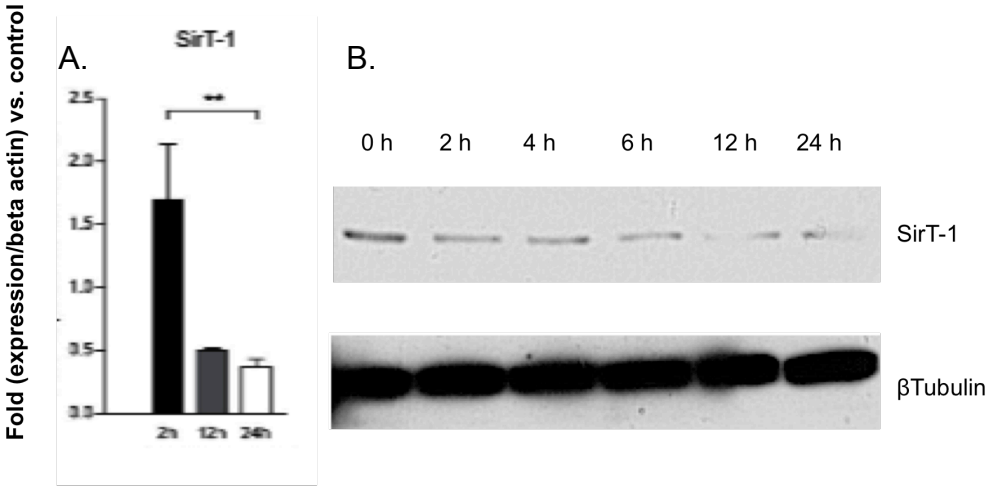

Figure 9. GnRH downregulates SirT-1.
Cells were treated with 10nM GnRH after overnight starvation. A.QPCR analysis of SirT-1 mRNA fold expression is normalized to non-treated cells. B. Protein levels of SirT-1 with GnRH stimulation of the following time points: 2 h, 4 h, 6 h, 12 h, 24 h.

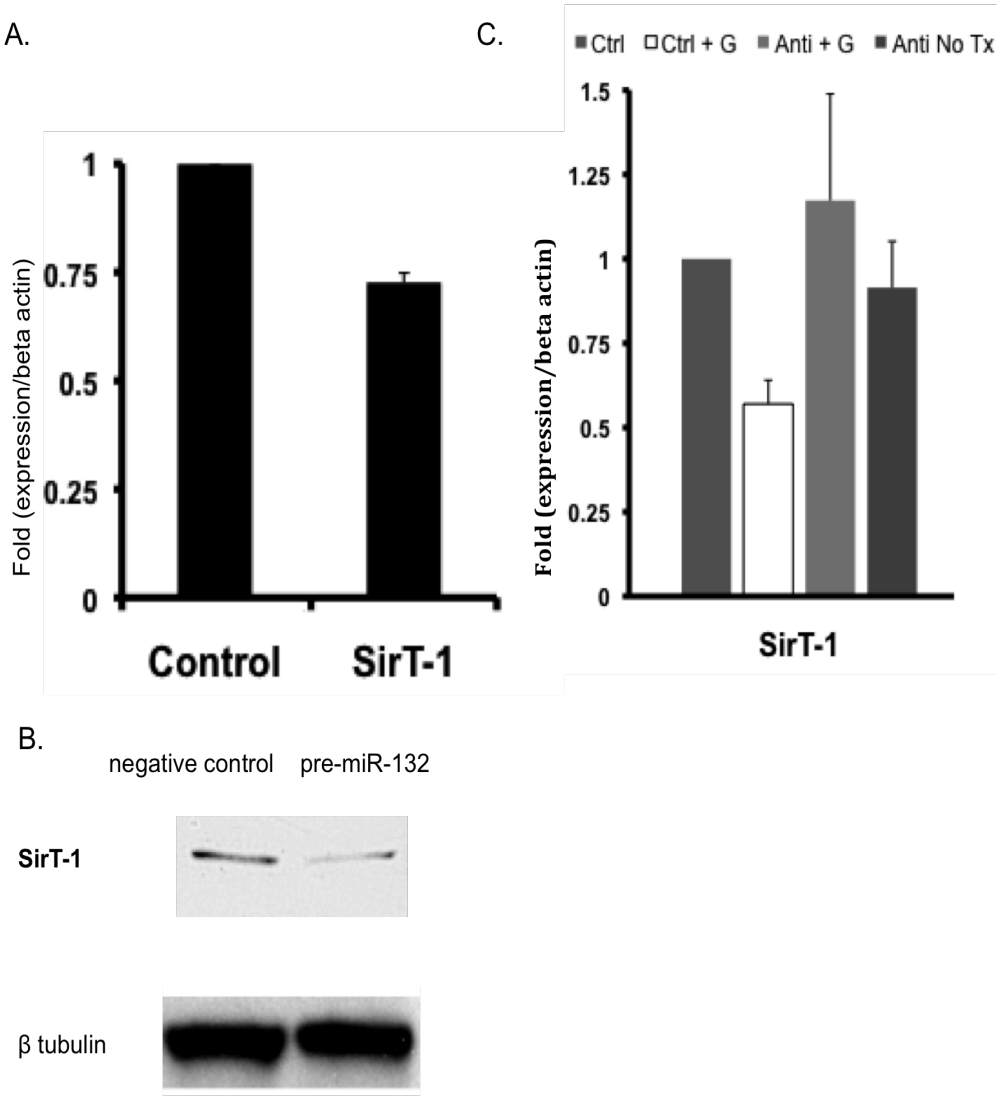

Figure 10. miR-132/212 mediates GnRH stimulated downregulation of SirT-1.

A. QPCR analysis of SirT-1 mRNA fold expression normalized to beta actin following pre-miR-132 transfection. B. Protein levels of SirT-1 of cells transfected with either negative control pre-miR or with pre-miR-132. C. QPCR analysis of SirT-1 mRNA fold expression normalized to beta actin following transfection with either anti-miR-132/212 or with negative control and either with or without 10 nM GnRH treatment.

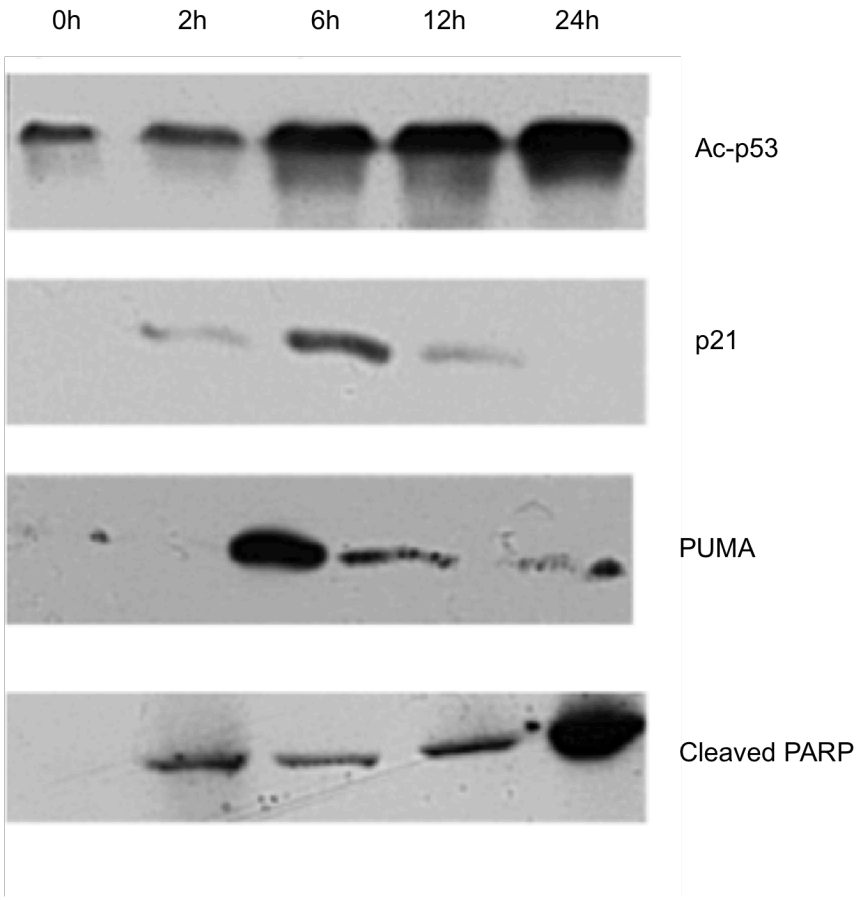

Figure 11. MiR-132/212 induces cell cycle arrest and apoptosis through SirT-1-p53 pathway.
GnRH increases p53 acetylation and induces p21 and PUMA, both peaking its levels at 6hr. PARP cleavage is also induced, peaking at 24 h post GnRH treatment

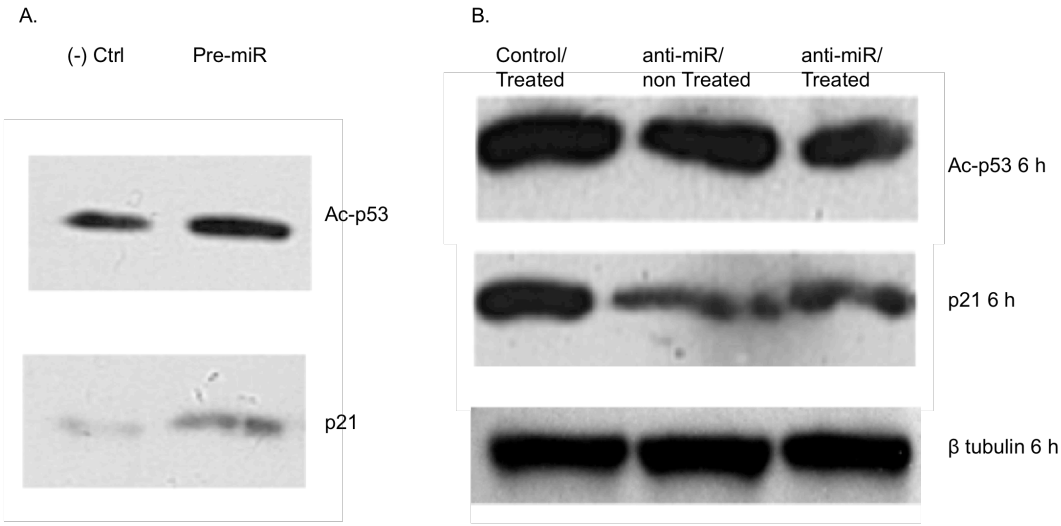

Figure 12. MiR-132/212 induces cell cycle arrest and apoptosis through SirT-1-p53 pathway.
A. Transfection with pre-miR-132 causes increase in p53 acetylation and p21 protein levels at 48 h post transfection. B. Transfection with anti-miR-132/212 blocks the GnRH stimulated acetylation of p53 and induction of p21 at 6 h post GnRH treatment.

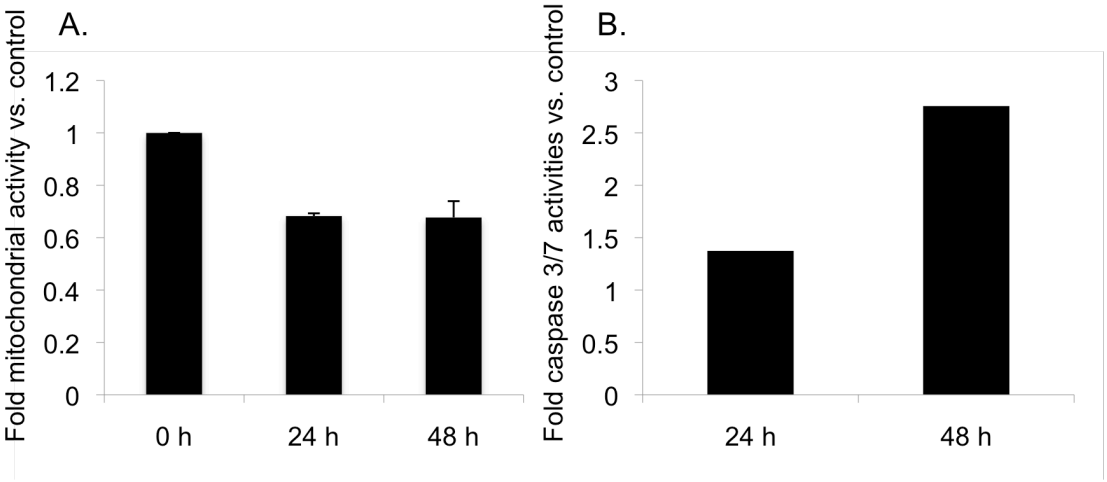

Figure 13. Reduction in proliferative activity and increase in apoptosis following pre-miR132 transfection.

A. Proliferative activity of cells following pre-miR132 transfection was assessed using CellTiter Aqueous Non-Radioactie Prolifeartion (MTS) Assay at 0, 24, and 48 h. As the data show, pre-miR transfected cells consistently showed lower viability than cells transfected with negative control pre-miR. (n=2) B. Apoptosis induced by pre-miR transfection was assessed using Apo-ONE Homogenous Caspase 3/7 Apoptosis Assay. Values are given in fold increase relative to negative control pre-miR. As shown, apoptosis is induced by pre-miR transfection at 24 and 48 h. (n=3)

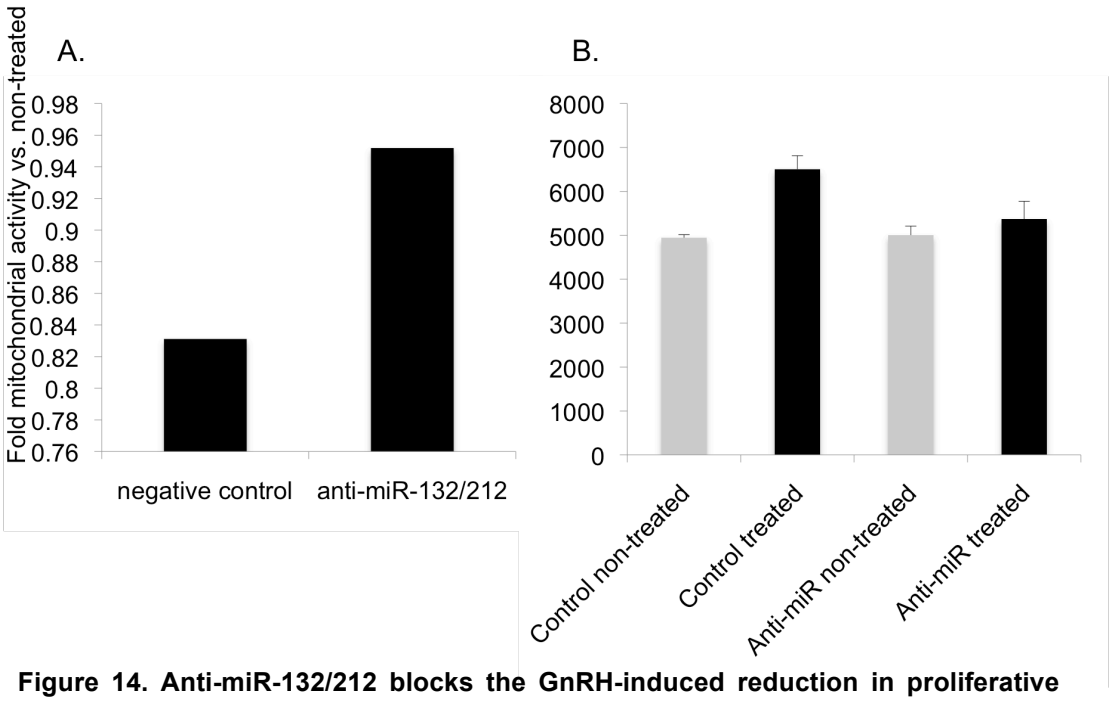

Figure 14. Anti-miR-132/212 blocks the GnRH-induced reduction in proliferative activity and increase in apoptotic activity.

A. Cells were first transfected with either anti-miR-132/212 or with negative control. Media was then changed to 0.5% FBS media with 10 nM GnRH or without and the proliferative activities of cells were assessed using CellTiter Aqueous Non-Radioactie Prolifeartion (MTS) Assay at 48 h. As the data show, anti-miR transfection blocks the GnRH-induced reduction in proliferation seen in cells transfected with negative control. (n=2) B. Cells were first transfected either with anti-miR-132/212 or with negative control. Media was then changed to 0.5% FBS meia with 10 nM GnRH or without and the activities of caspase 3/7 were measured using Apo-ONE Homogenous Caspase 3/7 Apoptosis Assay. Values are the average fluorescence reading values. As shown, GnRH induced apoptosis is blocked by anti-miR transfection at 48 h. (n=3)

REFERENCES

1. Lu M, Tang Q, Olefsky JM, Mellon PL, Webster NJG 2008. Adiponectin Activates Adenosine Monophosphate-Activated Protein Kinase and Decreases Luteinizing Hormone Secretion in LbetaT2 Gonadotropes. Molecular Endocrinology 22(3): 760-991

2. Tsutsumi R, Mistry D, Webster NJG 2010. Signaling Responses to Pulsatile Gonadotropin-releasing Hormone in LbetaT2 Gonadotrope Cells. The Journal of Biological Chemistry 285, 20262-20272

3. Knobil E 1974. On the control of gonadotropin secretion in the rhesus monkey. Recent Prog rom Res 30:1-46

4. Ciccone NA, Kaiser UB 2010. The Biology of Gonadotroph Regulation. Curr Opin Endocrinol Diabetes Obes. 16(4): 321-327

5. Finch AR, Caunt CJ, Armstrong SP, McArdle CA 2009. Plasma Membrane Expression of Gonadotropin-Releasing Hormone Receptors: Regulation by Peptide and Nonpeptide Antagonists. Molecular Endocrinology 24(2): 423-435

6. Shacham S, Cheifetz MN, Lewy H, Ashkenazi IE, Becker OM, Seger R. 1999. Mechanism of GnRH receptor signaling: from the membrane to the nucleus. Ann d'endo. 60(2):79-88.

7. Song SB, Rhee M., Roberson MS, Maurer RA, Kim KE. 2003. Gonadotropin-releasing hormone-induced stimulation of the rat secretogranin II promoter involves activation of CREB. Mol Cell Endo. 199 (1-2), pp. 29-36.

8. Ando H, Hew CL, Urano A. 2001. Signal transduction pathways and transcription factors involved in the gonadotropin-releasing hormone-stimulated gonadotropin subunit gene expression. Comparative Biochemistry and Physiology - B Biochemistry and Molecular Biology, 129 (2-3), pp. 525-532.

9. Gonzalez GA, Montminy MR. 1989. Cyclic AMP stimulates somatostatin gene transcription by phosphorylation of CREB at serine 133. Cell, 59 (4), pp. 675-680.

10. Lonze, BE, Ginty DD. 2002. Function and regulation of CREB family transcription factors in the nervous system Neuron, 35 (4): 605-623.

11. Purwana IN, Kanasaki H, Oride A, Miyazaki K. 2010. Induction of Dual Specificity Phosphatase 1 (DUSP1) by Gonadotropin-Releasing Hormone (GnRH) and the Role for Gonadotropin Subunit Gene Expression in Mouse Pituitary Gonadotroph LbetaT2 Cells. Biology of Reproduction, vol. 82 no. 2 352-362

12. Lewis BP, Shih IH, Jones-Rhoades MW, Bartel DP, Burge CB. 2003. Prediction of mammalian microRNA targets. Cell 115: 787-798.

13. Hutvagner G, Simard MJ. 2008. Argonaute proteins: key players in RNA silencing. Nat Rev Mol Cell Biol; 9: 22-32.

14. Brennecke J, Stark A, Russell RB, Cohen M. 2005. Principles of microRNA-target recognition. PLoS Biol. 2005 March; 3(3): e85.

15. Lewis BP, Burge CB, Bartel DP 2005. Conserved seed pairing flanked by adenosines, indicates that thousands of humangenes are microRNA targets. Cell 120, 15-20.

16. Turgeon JL, Kimura Y, Waring DW, Mellon PL 1996. Steroid and pulsatile gonadotropin-releasing hormone (GnRH) regulation of luteinizing hormone and GnRH receptor in a novel gonadotrope cell line. Molecular Endocrinology 10: 459-450

17. Turgeon JL, Windle JJ, Whyte DB, Mellon PL 1994. GnRH and estrogen regulate secretion of LH from an immortal gonadotrope cell line. Program of the 76th Annual Meeting of the Endocrine Society, Anaheim, CA (Abstract 1781)

18. Zhang H, Bailey JS, Coss D, Lin B, Tsutsumi R, Lawson MA, Mellon PL, Webster NJG 2006 Activin Modulates the Transcriptional Response of LßT2 Cells to gonadotropin-releasing hormones and alters Cellular Proliferation. Mol Endo 20(11):2909-2930

19. Shacham S, Harris D, Ben-Shlomo H, Cohen I, Bonfil D, Przedecki F, Lewy H, Ashkenazi IE, Seger R, Naor Z 2001. Mechanism of GnRH receptor signaling on gonadotropin release and gene expression in pituitary gonadotrophs. Vitam. Horm. 63: 63-90.

20. Brown G, Hughes PJ, Michell RH 2003. Cell differentiation and proliferation-simultaneous but independent? Experimental Cell Research. Volume 291, Issue 2, 10 December 2003, Pages 282-288

21. Wyllie AH. 2010 “Where, O death, is thy sting?” a brief review of apoptosis biology. Mol Neurobiol; 42(1):4-9

22. Hiroi H, Christenson LK, Chang L, Sammel MD, Berger SL, Strauss JF, 3rd 2004. Temporal and spatial changes in transcription factor binding and histone modifications at the steroidogenic acute regulatory protein (stAR) locus associated with stAR transcription. Mol Endo 18: 791-806.

23. Vo N, Kleim M, Varlamova O,Keller DM, Yamamoto T, Goodmn RH, Impey S 2005. A cAMP-response element binding protein-induced microRNA regulates neuronal morphogenesis. PNAS 102(45): 16426-16431.

24. Chen D, Pacal M, Wenzel P, Knoepfler P, Leone G, Bremner R 2010. Division and apoptosis and E2F-deficient retina Nature. 2009 December 17; 462 (7275): 925

25. Solomon JM, Pasupuleti R, Xu L, McDonagh T, Curtis R, DiStefano PS, Huber LJ 2006. Inhibition of SIRT1 catalytic activity increases p53 acetylation but does not alter cell survival following DNA damage Mol Cell Biol. 2006 January; 26(1): 28-38

26. Vogelstein B, Jane D, Levine AJ 2000. Surfing the p53 network Nature 208, 307 – 310 (16 November 2000)

27. Storer NY, Zon LI 2010. Zebrafish Models of p53 Functions Cold Spring Harbor Perspectives in Biology. May 5, 2010, doi: 10.1101/cshperspect.a001123

28. Remenyi J, Hunter CJ, Cole C, Ando H, Impey S, Monk CE, Martin KJ, Barton GH, Hutvagner G, Arthur JSC Regulations of the miR-212/132 locus by MSK1 and CREB in response to neurotrophins Biochem. J. (2010) 428, 281-291

29. Taganov KD, Bolding MP, Chang KJ, Baltimore D 2006. NF-κB-dependent induction of microRNA miR-146, an inhibitor targeted to signaling proteins of innate immune responses. Proc. Natl. Acad. Sci. USA. 103, 12481-12486

30. Brock M, Trenkmann M, Gay RE, Michel BA, Gy S, Fischler M, Ulrich S, Speich R, Huber LC 2009 Interleukin-6 modulates the expression of the bone morphogenic protein receptor type II through a novel STAT3-microRNA cluster 17/92 pathway Circ. Res. 104, 1184-1191

31. Yuen T, Ruf F, Chu T, Sealfon SC 2008 Microtranscriptome regulation by gonadotropin-releasing hormone Mol. Cel. Endo. 302 (2009) 12-17

32. Vo N, Klein ME, Varlamova O, Keller DM, Yamamoto T, Goodman RH, Impey S 2005. A cAMP-response element binding protein-induced microRNA regulates neuronal morphogenesis. Proc. Natl. Acad. Sci. U.S.A. 102, 16426-16431

33. Cheng HY, PappJW, Varlamove O, Dziema H, Russel B, Curfman JP, Nakazawa T, Shimizu K, Okamura H, Impey S, Obrietan K 2007. microRNA modulation of circadian-clock period and entrainment. Neuron 54, 813-829

34. Li Y, Matsumori H, Nakayama Y, Osaki M, Kojima H, Kurimasa A, Ito H, Mori S, Katoh M, Oshimura M, Inoue T 2010 SirT1 down-regulation in HeLa can induce p53 accumulation via p38 MAPK activation-dependent p300 decrease, eventually leading to apoptosis. Genes to cells:devoted to molecular and cellular mechanisms (9 November 2010) doi: 10.1111/j.1365-2443.2010.01460.x